

Constraining an Early Dark Energy Motivated Quintessential α -Attractor Inflaton Potential

Arunoday Sarkar and Buddhadeb Ghosh

Centre of Advanced Studies, Department of Physics, The University of Burdwan,
Burdwan 713 104, India

E-mail: adsarkar@scholar.buruniv.ac.in, bghosh@phys.buruniv.ac.in

Abstract. We construct a new model of quintessential α attractor inflation in conjunction with the features of non-oscillating early dark energy (EDE). Slow-roll plateau of this model is obtained, and analyzed in k -space, through the inflaton field and its first-order perturbation over a quasi de-Sitter metric fluctuation in the range $k = 0.001 - 0.009 \text{ Mpc}^{-1}$. The estimated cosmological parameters are found to obey Planck+BICEP2/Keck bounds with 68% CL with the required trend of spectral tilts in the $n_s - r$ parametric space. We verify that, the inclusion of the EDE does not significantly affect the observed parameters. Its presence manifests in obtaining *improved values* of the energy scale of inflation (M) and the present-day vacuum density (V_Λ). They are found to be $M = 5.58 \times 10^{-4} - 4.57 \times 10^{-3} M_P$ and $V_\Lambda = 1.042 \times 10^{-119} - 4.688 \times 10^{-116} M_P^4$. However, the α -parameter is drastically constrained in two ways. Its lower end is fixed by the consistency analysis of the k -mode equations, while the upper end is evaluated as a derived expression of α -cut-off through the aspects of EDE *viz.*, the effects of *Enhanced Symmetry Point* (ESP) in the potential during inflation. Improvised range of α is found to be $0.001 \leq \alpha < 0.1$ for the model parameters γ and n lying within $0.01 \leq \gamma \leq 0.09$ and $8 \leq n \leq 10$ respectively. These ranges are shown to be essential for satisfying the COBE/Planck normalized energy scale of inflation and the Planck-value of present-day vacuum density. If we choose $\gamma = 0.0818$ and $n = 8$, then we get $0.001 \leq \alpha \leq 0.0186$. Thus, the lower and upper limits of α are diminished substantially, compared with those in the earlier studies. We also argue that, the lower values of α can be instrumental in resolving the H_0 -discrepancy, whereas its higher values are capable of explaining both the early- and the late-time expansions of the universe, as discussed in some current literature.

Contents

1	Introduction	1
2	EDE-motivated quintessential α-attractor (EMQA) model	3
3	Quantum treatment of perturbation during inflation and associated parameters — a very brief overview	11
3.1	Quasi de-Sitter Hubble-exit of the dynamical inflaton modes and their evolutions	12
3.2	Inflationary parameters for EMQA model	13
4	Results and discussions	17
4.1	Prerequisites	17
4.2	Inflaton field and its first order perturbation	20
4.3	Mode responses of the parameters during EMQA-inflation	21
4.4	Role of ESP in constraining the parameter α	33
4.5	Obtained results in light of PLANCK-2018	36
4.6	A remark on the resolution of the Hubble tension	38
5	Conclusions	39

1 Introduction

One of the great achievements of Λ -cold dark matter (Λ CDM) model is to identify the major component [1] of our universe, *viz.*, the ‘dark energy’ (DE) [2]. The current accelerating expansion of the universe, which is confirmed by several cosmological surveys, based on redshift observations [3, 4], cosmic microwave background (CMB) anisotropies plus polarization sky-maps [1, 5–8] and various other astrophysical explorations [9, 10] supports the existence of DE, having barotropic parameter $\omega = -1.03 \pm 0.03$ [7]. One way of elucidating this exotic element is to introduce a new scalar field, the ‘quintessence’¹ [11–14] in order to solve the *cosmological constant problem* [15, 16]. The quintessential scalar field is unique in so far as other models of DE are concerned, because it is characterised by a variable barotropic parameter in the range $-1 \leq \omega \leq -0.95$ [7]. However, the quintessence proposition has its own internal inconsistencies, especially regarding its initial conditions. This is known as the *coincidence problem* [16–22]. It is required to merge coherently with the inflaton field to address both the early and the late-time expansions of the universe, along with the period of *kination* [23–26] within a single unified framework, *viz.*, the *quintessential inflation* [27–88].

Despite being so successful, the Λ CDM model, which is a standard theoretical tool for understanding the present universe from first few seconds until today, is not yet complete. There are two missing links *viz.*, the *Hubble tension* [89–105] and the σ_8 *discrepancy*² [99–101, 104, 106–112].

Cosmological parameters, specifically the observed expansion rate and the current age of the universe are estimated by the precise measurement of Hubble constant H_0 . Various processes to determine H_0 can be broadly categorized into two major classes [113]: (i)

¹considered to be the fifth element after normal baryonic matter, dark matter, photon and neutrino.

²related to the dark matter-dark energy interactions and the matter clustering processes.

Analysis of the fluctuations in cosmic microwave background radiation (CMBR) at redshift $z = 1089.80 \pm 0.21$ [7] (at the last scattering surface) (or from the Baryon Acoustic Oscillations (BAO)) by the Planck satellite [7]; (ii) The cosmic distance ladder (CDL) methods such as redshift observations [89, 90] of distant type-1a supernovae or Cepheid stars at redshift $z = \mathcal{O}(1)$. However, there is a 5σ level disagreement³ between the values of H_0 , obtained by these two methods. The value given by Planck [7] is

$$H_0^{\text{Planck}} = 67.44 \pm 0.58 \text{ Km s}^{-1}\text{Mpc}^{-1} \quad (1.1)$$

whereas the CDL measurement from Cepheid-SN-1a by SH0ES collaboration [115] gives

$$H_0^{\text{SN}} = 73.04 \pm 1.04 \text{ Km s}^{-1}\text{Mpc}^{-1}. \quad (1.2)$$

Many possible resolutions of the discrepancy between these two values have been discussed in Refs. [116–121]. Most of them rely on early universe phenomenology.

In many contemporary literature [93, 113, 122–165] it has been suggested that a viable option to alleviate the 5σ tension is to propose a new version of dark energy, the *Early Dark Energy* (EDE)⁴ during matter-radiation equality without any substantial modification of Λ CDM. The cosmological parameters which are tightly constrained by the Planck observations remain unaltered by the EDE. Actually, the EDE is formulated in such a way [116, 120, 121] that its decay rate is faster than the background energy density (particularly the radiation⁵) [123], so that its effects can not be tested in CMB observations. However, according to Friedmann equations the value of H_0 can be lifted slightly by the increase in the overall density of the universe, induced by the EDE. This has been shown to be possible by considering either a first order phase transition [138] or an EDE oscillation [120, 122, 123, 138–145] near the potential minimum.

Recently, the EDE has been considered [113] to be a promising candidate for resolving the H_0 tension in the quintessential form of the α -attractor potential. In this model, the EDE is identified with a scalar field of non-oscillating (NO) type near the matter-radiation equality at the Enhanced Symmetry Point (ESP) [166, 167], present in the potential profile, which can decay faster than the oscillating one [145] and is believed to be the fastest, that is possible [113]. In this work [113], the authors perform a simulation, engaging the Friedmann equations, the Klein-Gordon equation and the continuity equations for radiation and matter, with the conditions from matter-radiation equality, decoupling and the present values of various cosmological parameters. The results of the simulation process reveal that within reasonable choices of the parameter space, the model yields required constraints for post-inflationary as well as for the current DE-related observations. We feel, in order to make the outcome of this survey more concrete, the scenario should be connected with the inflationary paradigm *vis-à-vis* the microscopic mode behaviour of the inflaton field and the relevant cosmological parameters.

In a previous work [168], we made a quite similar kind of study. There, the inflationary slow-roll regime was probed for a specific class of quintessential α -attractor models through a sub-Planckian k -space first order quantum mode analysis in the background of a quasi

³Actually it is in between 4.56σ and 6.36σ [114].

⁴The connotation ‘*early*’ is used to differentiate it from the usual one which is responsible for the present accelerated expansion of the universe.

⁵The decay is so rapid that the EDE fades away before the decoupling of CMB photon from the last scattering surface.

de-Sitter metric fluctuation, developed in Ref. [169], under spatially flat gauge. The self-consistent solutions for $k = 0.001 - 0.009 \text{ Mpc}^{-1}$ revealed that the relevant cosmological parameters agree with the Planck-2018 data very well within a given range and accuracy. Specifically, the cumulative mode responses of the scalar spectral index (n_s) and the tensor-to-scalar ratio (r) showed that the spectral tilts obeyed the Planck bounds with 68% CL, which eventually constrain the model parameters as $n = 122$ and $\frac{1}{10} \leq \alpha \leq 4.3$ continuously. It was found that, below $\alpha = \frac{1}{10}$ the evolution equations are insensitive to α and beyond $\alpha = 4.3$ no convergence is observed for obtaining a consistent solution. Four values of α *viz.*, $\alpha = 1/10, 1/6, 1$ and 4.3 were chosen for which the slow-roll plateau with the inflationary energy scales $M = 4.28 \times 10^{15} - 1.11 \times 10^{16} \text{ GeV}$ was found to satisfy COBE/Planck normalisation and the quintessential tail part yielded dynamically the present day vacuum density with the amplitude $V_\Lambda \approx 10^{-115} - 10^{-117} M_P^4$. We also compared our results with ordinary α attractor E and T models and discovered that the quintessence always restricts the potential to be single-field concave type and prevents its mutation into the simple chaotic one which is ruled out by Planck, thereby making the concerned model just appropriate for quintessential inflation.

In the present paper, we make a connection of our earlier work [168] to the EDE proposal. Our primary focus will be on further constraining the important parameter α using the EDE as a tool in the light of Planck-2018 data. We therefore extend the formalism developed in Ref. [168] keeping in mind the aspects of EDE in the inflaton potential.

The paper is organised in this way. In Section 2, we set up our model in non-canonical and canonical field spaces, describe its pole behaviour, study the EDE dynamics and display the variations of the obtained potential with respect to the model parameters. Section 3 outlines the quasi de-Sitter Hubble-exit of the quantum inflaton modes and their evolutions with a brief introduction of the relevant cosmological parameters. The corresponding boundary conditions and the mode responses of the parameters are illustrated in Section 4. Then in the same section we constrain the parameter α by the mode equations in conjunction with the EDE. In this course, we find that the lower values of α fit the Planck data in improved way. We use these results to make a comparative study with the Planck+BICEP2/Keck bounds and then write a brief discussion here regarding further constraining the ranges of the model parameters, which could be helpful in resolution of the Hubble tension. Finally Section 5 contains some concluding remarks.

2 EDE-motivated quintessential α -attractor (EMQA) model

We consider the action,

$$S_{\text{minimal}}[x] = \int_{\Omega} d^4x \sqrt{-g(x)} \left[\frac{1}{2} R(x) + \mathcal{L}_{\text{non-canonical}}(\theta(x), \partial\theta(x)) \right] \quad (2.1)$$

of a non-canonical inflaton field θ measured in the reduced Planck scale, $M_P = (8\pi G)^{-1/2} = 2.43 \times 10^{18} \text{ GeV}$, minimally coupled with gravity, whose symmetry and dynamics are controlled by the Lagrangian⁶ [113]

$$\mathcal{L}_{\text{non-canonical}}(\theta, \partial\theta) = - \left[1 - \frac{\theta^2}{(\sqrt{6}\alpha M_P)^2} \right]^{-2} \frac{g^{\mu\nu} \partial_\mu \theta \partial_\nu \theta}{2} - V(\theta). \quad (2.2)$$

⁶The Lagrangian is written following the metric signature $(-, +, +, +)$.

The kinetic part of Eq. (2.2) contains the same non-trivial quadratic pole structure of quintessential α -attractor inflation as described in detail in Ref. [168]. The poles at $\theta = \pm\sqrt{6}\alpha M_P$ save the model from the issues arising from the super-Planckian effects like the ‘*fifth force problem*’ [16, 71, 170] and the radiative corrections [171–173] due to infinite field excursion of the non-canonical scalar field θ , which therefore ensure that the inflaton field behaviour near the pole boundary is genuinely sub-Planckian. In Ref. [168] it was discussed that the presence of these non-canonical poles is in fact a generic feature of α -attractors [174–189] in the context of ‘*pole inflation*’ in $\mathcal{N} = 1$ minimal supergravity and exclusive as well, because such poles are not generally found even in string theory [190–192].

So far as the potential part⁷ is concerned, we take,

$$V(\theta) = \exp\left(\gamma e^{-\sigma\sqrt{6}\alpha}\right) M^4 \exp\left(-\gamma e^{-\frac{\sigma\theta}{M_P}}\right). \quad (2.3)$$

Eq. (2.3) is radically different from what is considered in [168]. The double exponential structure is a modification over the simple ‘exp’ type of potential in quintessential inflation such that it can embed the EDE smoothly in the field dynamics. γ and σ are the dimensionless positive constants which can deform the shape of the potential substantially. This will be seen shortly. However, the most valuable parameter here is α , which is the characteristic constant of the well known α -attractor formulation, signifying the reciprocal curvature of the underlying $SU(1,1)/U(1)$ Kähler manifold,

$$\alpha = -\frac{2}{3\mathcal{R}_{\mathcal{K}}}. \quad (2.4)$$

Optimising the value of α is indispensable in the assimilation of several theoretical [193–200] as well as experimental aspects [7, 8, 201–203] in conjunction with the various cosmological observations regarding CMB B -mode polarization [7, 8, 201–203], gravitational waves [71] and the stage III/IV DE and large scale structure (LSS) surveys [66–69].

In Ref. [169], we analysed the quantum modes of the linear inflaton perturbation in $k \rightarrow 0$ limit incorporating the primitive forms of the α -attractor E and T models and the results showed that for $\alpha_E = 1, 5, 10$; $\alpha_T = 1, 6, 10$ (with 68% CL) and $\alpha_{E,T} = 15$ (with 95% CL) for the exponent $n = 2$; and $\alpha_E = 1, 6, 11$ and $\alpha_T = 1, 4, 9$ for $n = 4$ (with 68% CL), the E/T models can explain all the necessary constraints of the Planck-2018 data. Similarly in Ref. [168] it was discovered that attaching quintessence with the α -attractor framework, the α values are diminished considerably into the closed interval $0.1 \leq \alpha \leq 4.3$ for a large power $n = 122$ to accommodate both the early and the late-time expansions of the universe. Now, it will be worthwhile to explore the behaviour of α when we equip the potential with EDE in addition to DE. This might bear some clues regarding further understanding of EDE. With this objective, we present below some related derivations.

The potential in Eq. (2.3) has two asymptotic limits, as the field θ approaches the poles

⁷The structure of the potential is inspired by that in Ref. [113]. Because it shows that such a functional dependence is efficient in resolving the Hubble tension. In this paper, the structure of the potential is slightly customized in comparison with that in [113] to incorporate both inflation and quintessence. Our aim is to construct a model which can accommodate inflation, quintessence as well as EDE.

of the inflaton-kinetic term in Eq. (2.2):

$$\begin{aligned}
\lim_{\theta \rightarrow +\sqrt{6\alpha}M_P} V(\theta) &= \exp\left(\gamma e^{-\sigma\sqrt{6\alpha}}\right) M^4 \exp\left(-\gamma e^{-\sigma\sqrt{6\alpha}}\right) \\
&= \exp\left[-\gamma\left(e^{-\sigma\sqrt{6\alpha}} - e^{-\sigma\sqrt{6\alpha}}\right)\right] M^4 \\
&= M^4
\end{aligned} \tag{2.5}$$

and

$$\begin{aligned}
\lim_{\theta \rightarrow -\sqrt{6\alpha}M_P} V(\theta) &= \exp\left(\gamma e^{-\sigma\sqrt{6\alpha}}\right) M^4 \exp\left(-\gamma e^{\sigma\sqrt{6\alpha}}\right) \\
&= \exp\left[-\gamma\left(e^{\sigma\sqrt{6\alpha}} - e^{-\sigma\sqrt{6\alpha}}\right)\right] M^4 \\
&= \exp\left[-2\gamma \sinh\left(\sigma\sqrt{6\alpha}\right)\right] M^4 \\
&= V_\Lambda.
\end{aligned} \tag{2.6}$$

These two extreme limits indicate the energy scales of inflation M ($\sim 10^{15}$ GeV) and the present day vacuum density V_Λ of the universe ($\sqrt[4]{V_\Lambda} \sim 10^{-12}$ GeV) [7, 8] respectively.

Now, we redefine the inflaton field as,

$$\xi = \sqrt{6\alpha}M_P \tanh^{-1}\left(\frac{\theta}{\sqrt{6\alpha}M_P}\right) \tag{2.7}$$

in such a way that the non-canonical kinetic term transforms into a canonical one as

$$-\left[1 - \frac{\theta^2}{(\sqrt{6\alpha}M_P)^2}\right]^{-2} \frac{g^{\mu\nu}\partial_\mu\theta\partial_\nu\theta}{2} = -\frac{1}{2}\partial_\mu\xi\partial^\mu\xi \tag{2.8}$$

from which we obtain a new form of the quintessential α -attractor inflaton potential

$$V(\xi) = \exp\left(\gamma e^{-\sigma\sqrt{6\alpha}}\right) M^4 \exp\left(-\gamma e^{-\sigma\sqrt{6\alpha} \tanh\left(\frac{\xi}{\sqrt{6\alpha}M_P}\right)}\right). \tag{2.9}$$

We can express this potential in a more convenient form by defining a power index $n = \sigma\sqrt{6\alpha}$

$$V(\xi) = \exp(\gamma e^{-n}) M^4 \exp\left(-\gamma e^{-n \tanh\left(\frac{\xi}{\sqrt{6\alpha}M_P}\right)}\right). \tag{2.10}$$

This newly obtained potential features identical pole behaviours as that of Eq. (2.3) with the correspondences

$$\lim_{\xi \rightarrow +\infty} V(\xi) \implies \lim_{\theta \rightarrow +\sqrt{6\alpha}M_P} V(\theta) = M^4 \tag{2.11}$$

and

$$\lim_{\xi \rightarrow -\infty} V(\xi) \implies \lim_{\theta \rightarrow -\sqrt{6\alpha}M_P} V(\theta) = V_\Lambda, \tag{2.12}$$

following Eq. (2.7). In this new version of the potential, the poles at $\theta = \pm\sqrt{6\alpha}M_P$ are stretched to $\xi = \pm\infty$ and the boundaries of these poles manifest as the inflationary plateau and the quintessential tail in the positive and negative limits, respectively.

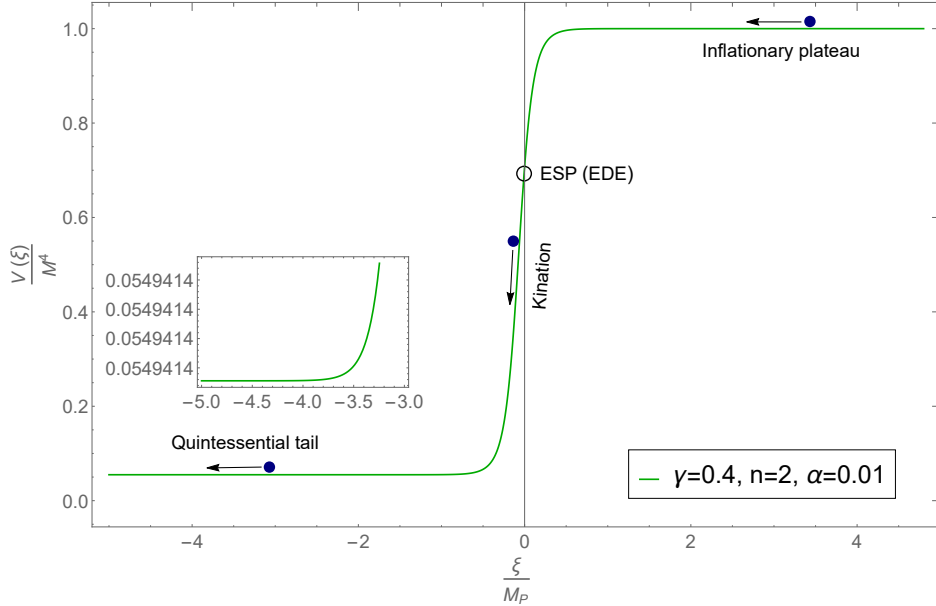


Figure 1. Graphical representation of the potential of Eq. (2.10) for $\gamma = 0.4$, $n = 2$ and $\alpha = 0.01$, as an example. These values are chosen to show the important phases of the quintessential inflation with EDE. The inflaton field starts its journey over the slow-roll plateau from infinity (or from the pole in non-canonical field space). When it reaches the ESP at origin, indicated by the ring with a positive energy $V(0)$, it gets stuck for a while due to an interaction with some other heavy fields. It remains frozen there until matter-radiation equality when its density parameter reaches a maximum value before decoupling. The time of freezing is actually fixed by the interaction time plus the time required for the decay of the additional particles. Then it experiences the sharp gradient of the potential and the field energy drains away to a negative value at the throat of the quintessential runaway. As long as the field remains frozen at the ESP, the field acts as an early version of the dark energy without disturbing the Λ CDM parameters at all. It doesn't even leave any traces in CMBR, such that the observations can not detect its presence in the background. When the period of kination terminates, the field enters into the final part of the potential to serve the late-time expansion of the universe in the form of DE with energy much smaller than that of the inflationary one.

In figure 1 we depict the potential of Eq. (2.10) normalized by M^4 against the canonical field ξ in unit of M_P for three sample model parameters *viz.*, $\gamma = 0.4$, $n = 2$ and $\alpha = 0.01$. The inflaton field, denoted by the blue ball starts rolling slowly from $\xi > 0$ region over the inflationary plateau with a significant amount of energy ($\sim 10^{15}$ GeV) against the Hubble drag. As a result, the potential energy dominates over the kinetic one until the field reaches a point where the first slow-roll parameter ϵ_V is unity. It is the place where the inflation ends and after that, the field enters into a new region, called '*kination*'. Generically, this phase is characterized by a fast decay rate (possibly fastest [113]) of the energy density of the field $\rho_\xi \propto \frac{1}{a^6}$ [16] with scale factor a and eventually the field undergoes a kinetically driven free-fall until it moves towards $\xi < 0$ region and resurrects as DE in the form of quintessence [63] with the energy $\sim 10^{-12}$ GeV, as we observe today. But, here the scenario is strikingly different, rather novel.

The potential considered in Eq. (2.3) or (2.10) has a new feature, called the '*Enhanced Symmetry Point (ESP)*' [113, 166, 167] at $\theta = 0$ (or, $\xi = 0$) (shown by a ring in figure 1). Thus, when the field hits the origin, it gets trapped due to a quadratic interaction with some other heavy fields *viz.*, the Θ particles of type $\delta V_{\text{int}}(\theta, \Theta) = \frac{1}{2}p^2\theta^2\Theta^2$ for the coupling

strength $p < 1$ [16, 113, 166, 167, 204]. As a result, all the kinetic energy of the ξ -field (or θ field) developed during traversing from the end of inflation to the origin, is transferred to Θ particles, and the θ field (or the ξ field) sticks at the origin with constant potential energy density $V(0)$ *vis-à-vis* a fixed (total) energy density $\rho_\xi(0)$. On the other hand, in the background, the Θ particles being massive decay into matter and radiation in the thermal bath of the hot big bang (HBB) [16, 113, 167]. The densities of matter (ρ_{matter}) and radiation (ρ_{rad}) then start to decrease with scale factor as $\rho_{\text{matter}} \propto a^{-3}$ and $\rho_{\text{rad}} \propto a^{-4}$ [16, 205, 206], diminishing the total background energy density ($\rho_{\text{matter}} + \rho_{\text{rad}}$) of the universe. As radiation density decreases faster than the matter density, at a particular scale factor, the two densities will be equal, called the *matter-radiation equality* at redshift $z_{\text{equal}} = 3387.4$ [7].

Now, from the starting of production of matter and radiation to the matter-radiation equality, as the total density of the universe in the background decreases, the density parameter of the ξ -field at origin (*i.e.* at the ESP) $\Omega(\xi = 0) = \frac{\rho_\xi(0)}{\rho_{\text{matter}} + \rho_{\text{rad}}}$ increases and attains a maximum value Ω_{equal} at the instant of equality. According to Refs. [14, 16, 113, 207], when the density parameter of ξ -field becomes maximum, the frozen scalar field unfreezes before dominating. Afterward, the ξ -field faces the steepest section of the potential due to the exp (exp) structure of the potential and freely falls to a negative value $-\frac{\sqrt{48\alpha}}{n\gamma} M_P = -0.87 M_P$ (derived from an expression given in Ref. [113] for the dynamics of the field during free-fall and the model parameters chosen in figure 1) in the quintessential runaway. Then, it again refreezes at the potential minimum at a constant potential energy density comparable to the present-day density of matter until it becomes dominant in the present universe as dark energy, causing the observed late-time acceleration of the universe.

As long as the ξ -field stays frozen at the ESP ($\xi = 0$), its kinetic energy density is zero and potential energy density is constant at $V(0)$. Therefore, during this period of freezing the barotropic parameter of ξ -field is effectively (-1) , which is the same as that of dark energy. This indicates that starting from being trapped at the ESP to the matter-radiation equality, the ξ -field behaves like an early version of dark energy and hence the name: ‘*Early Dark Energy (EDE)*’. In this course, it contributes additional energy to the dark energy sector, which slightly hikes the expansion rate of the universe [140] in such a way that the value of H_0^{Planck} can be increased by 8.3% in order to match with the value of H_0^{SN} ⁸. Therefore, the scalar field ξ , which plays the roles of inflaton during slow-roll and DE at the present day, can also play another role, called EDE at ESP near matter-radiation equality before CMB decoupling. For more details see figure 9 of Ref. [113]. In this way, the idea of EDE shows an effective resolution of the Hubble tension. However, this change of the Hubble expansion does not calibrate the cosmological parameters of Λ CDM model constrained by Planck because the decay rate of the EDE field energy is so fast that its effect does not appear in the CMB anisotropies and polarizations [123]. Consequently, the EDE remains a hypothetical entity [113] whose apparent role is to tune the expansion to alleviate the H_0 discrepancy.

In the present work, we employ the above-mentioned aspects in constraining the model parameters, specifically the α , through a quantum dynamical mode analysis of the inflationary perturbations and the resulting cosmological parameter estimations, following the path of earlier studies [168, 169]. But, at first, we would like to study how the potential responds to the variations of its model parameters, which will guide us to pick up right choices of the parameter space for the subsequent analysis.

⁸Because $\frac{H_0^{\text{SN}} - H_0^{\text{Planck}}}{H_0^{\text{Planck}}} \times 100 \approx 8.3$.

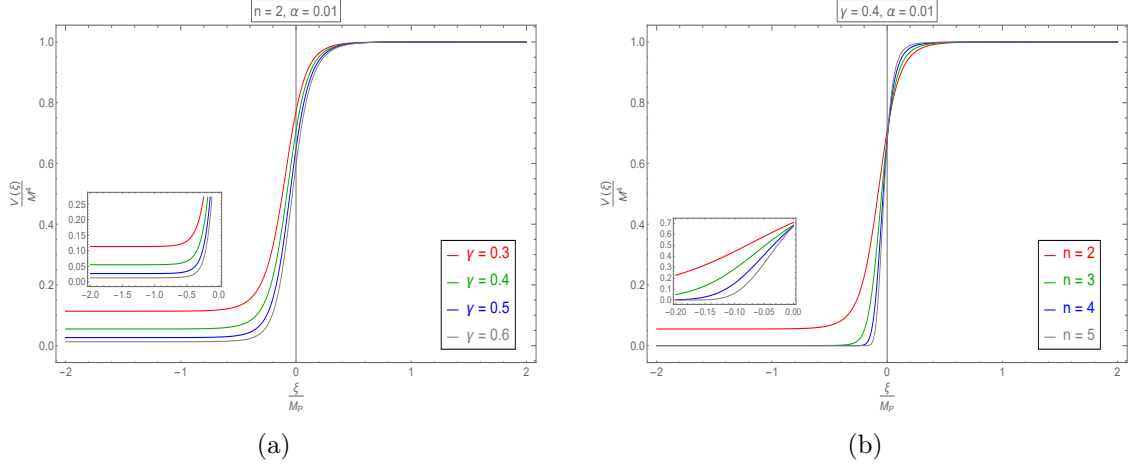


Figure 2. Figure 2a shows the dependence of the ESP with γ for $n = 2$ and $\alpha = 0.01$. As γ varies from $\gamma = 0.6$ to $\gamma = 0.3$ the point of freezing of EDE is uplifted, while in figure 2b it is almost unaltered with the change of n from $n = 2$ to $n = 5$ for $\gamma = 0.4$ and $\alpha = 0.01$. The high values of n play the major role to determine the correct slope of the potential compatible with the EDE-expansion of the universe. Thus small $\gamma (\ll 1)$ and large $n (> 1)$ together govern the overall shape of the required potential.

Figures (2a) and (2b) illustrate the changes in geometry and energy scales of the potential for variations in γ and n respectively, for a fixed value of α (here, $\alpha = 0.01$). The energy scale of inflation M , being independent of γ and n (see Eq. (2.5)), remains the same while that of quintessence, the $V_\Lambda = \exp(-2\gamma \sinh(n))M^4$ varies with n and γ (see Eq. (2.6)). Here, the noticeable fact is that when γ decreases from $\gamma = 0.6$ to $\gamma = 0.3$ in figure 2a, the ESP, $V(0) = \exp[-\gamma(1 - e^{-n})]M^4$ increases slowly. In figure 2b, the ESP is almost fixed by the variation of n for a given value of γ (here, $\gamma = 0.4$), because $[-\gamma(1 - e^{-n})] \approx (-\gamma)$ for $n > 1$. Actually the index n controls the steepness of the potential. As n increases from $n = 2$ to $n = 5$ the gradient increases, signifying faster and faster decay rate of the EDE field energy which is also an important criterion for the EDE dynamics. Therefore, slightly higher values of n are preferable. Now, if the potential is approximated near equality at origin, then we get,

$$\lim_{\xi \rightarrow 0} V(\xi) = \exp[-\gamma(1 - e^{-n})]M^4 \exp\left(\frac{n\gamma\xi}{\sqrt{6\alpha}M_P}\right). \quad (2.13)$$

Refs. [14, 113, 207] show that for such an approximate exponential dependence of the potential near equality (called the *exponential attractor* or *scaling attractor*), the density parameter of the field at equality takes the form

$$\Omega_{\text{equal}} \simeq \frac{18\alpha}{(n\gamma)^2} < 1. \quad (2.14)$$

Therefore, for a fixed value of Ω_{equal} , slightly high value of n corresponds to a small value of γ , which are the necessary conditions for the successful model building of quintessential inflation with EDE. In fact, such choices of n and γ are consistent with the experimental bounds of energy scales of inflation and present-day vacuum density, which we shall explain in Section 4.

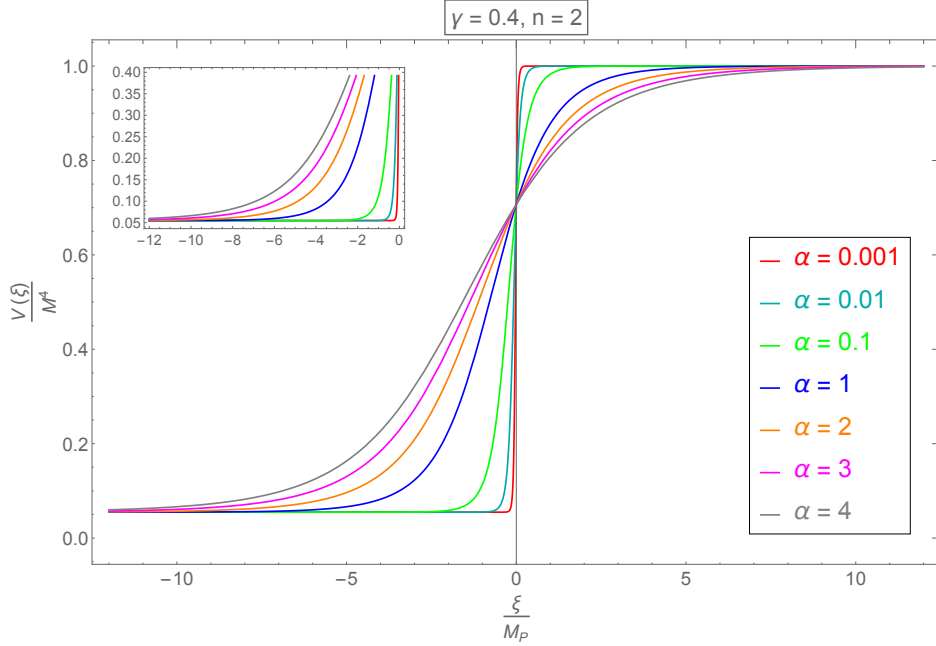


Figure 3. As α increases from $\alpha = 0.001$ to $\alpha = 4$ the potential is deformed from slow-roll to polynomial type. Low values of α ($\alpha < 1$) give steeper free-fall of the field compared to the high values of α ($\alpha > 1$). Therefore the fractional values of α are suitable for the framework of EDE in quintessential inflation.

The parameter set (n, γ) , is not adequate for fixing the energy densities M and V_Λ completely. An appropriate value of α is equally important here, not only for fitting the scales, but also for achieving a single-field model of concave type with a flat direction during inflation. In this context, figure 3 depicts the variation of the potential with α for $n = 2$ and $\gamma = 0.4$, for example. As α grows from $\alpha = 0.001$ to $\alpha = 4$, the potential shows the same double pole behaviour as that of ordinary α -attractor and quintessential α -attractor models, for which mode analyses were done in Refs. [168, 169] respectively. For the smaller values of α , the potential is highly concave resulting in an infinitely extended region over which the inflaton field rolls very slowly. As α crosses the value $\alpha \approx 0.1$, the potential loses its concave nature and starts to become convex of the simple polynomial-type chaotic inflation. This is one way of looking at the picture from the angle of inflation. We can also interpret the phenomenon in the perspective of EDE. When α is fractional, the potential shows a steeper slope, which is beneficial for the fast decay of the EDE energy, which does not appear in the CMBR [113]. Therefore, small fractional values of α are quite favourable for the EDE field dynamics in quintessential formulation of inflation. We shall further analyze these points in the sub-Planckian k -space analysis of the inflationary modes in Section 4 and understand that the ESP will restrict the allowed range of α more precisely.

It would be convenient to redesign the complicated potential of Eq. (2.10) into two simplified forms by successive approximations for two extreme limits of ξ (*i.e.* $\xi = \pm\infty$) corresponding to the inflationary plateau and quintessential tail. From Eq. (2.10) in $\xi \rightarrow +\infty$

we get,

$$\begin{aligned}
V(\xi) &= \exp(\gamma e^{-n}) M^4 \exp \left[-\gamma e^{-n \tanh\left(\frac{\xi}{\sqrt{6\alpha} M_P}\right)} \right] \\
&\approx \exp(\gamma e^{-n}) M^4 \exp \left[-\gamma e^{-n \left(1 - 2e^{-\sqrt{\frac{2}{3\alpha}} \frac{\xi}{M_P}}\right)} \right] \\
&\approx \exp(\gamma e^{-n}) M^4 \exp \left[-\gamma e^{-n} \left(1 + 2ne^{-\sqrt{\frac{2}{3\alpha}} \frac{\xi}{M_P}}\right) \right] \\
&\approx M^4 \left[1 - e^{-n} 2n\gamma \exp \left(-\sqrt{\frac{2}{3\alpha}} \frac{\xi}{M_P} \right) \right] \\
&= V_{\text{inf}}(\xi).
\end{aligned} \tag{2.15}$$

Similarly for $\xi \rightarrow -\infty$ gives,

$$\begin{aligned}
V(\xi) &= \exp(\gamma e^{-n}) M^4 \exp \left[-\gamma e^{-n \tanh\left(\frac{\xi}{\sqrt{6\alpha} M_P}\right)} \right] \\
&\approx \exp(\gamma e^{-n}) M^4 \exp \left[-\gamma e^{-n \left(-1 + 2e^{\sqrt{\frac{2}{3\alpha}} \frac{\xi}{M_P}}\right)} \right] \\
&\approx \exp(\gamma e^{-n}) M^4 \exp \left[-\gamma e^n \left(1 - 2ne^{\sqrt{\frac{2}{3\alpha}} \frac{\xi}{M_P}}\right) \right] \\
&\approx \exp[-\gamma(e^n - e^{-n})] M^4 \left[1 + e^n 2n\gamma \exp \left(\sqrt{\frac{2}{3\alpha}} \frac{\xi}{M_P} \right) \right] \\
&= \exp[-2\gamma \sinh(n)] M^4 \left[1 + e^n 2n\gamma \exp \left(\sqrt{\frac{2}{3\alpha}} \frac{\xi}{M_P} \right) \right] \\
&= V_{\Lambda} \left[1 + e^n 2n\gamma \exp \left(\sqrt{\frac{2}{3\alpha}} \frac{\xi}{M_P} \right) \right] \\
&= V_{\text{quint}}(\xi).
\end{aligned} \tag{2.16}$$

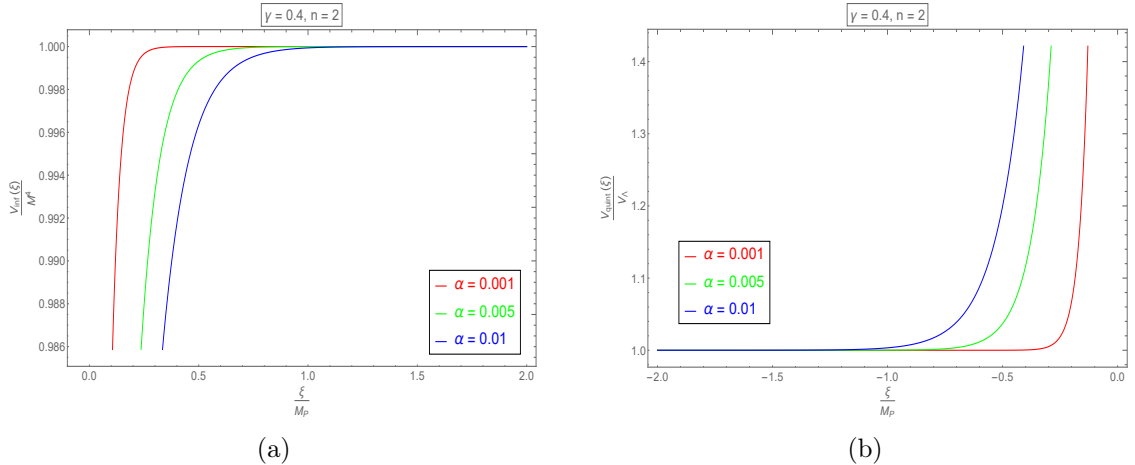


Figure 4. Approximated versions of Eq. (2.10) in $\xi \gg 0$ and $\xi \ll 0$ limits for $\gamma = 0.4$, $n = 2$ and $\alpha = 0.001, 0.005$ and 0.01 . Figure 4a corresponding to the former limit describes the simplified inflaton potential and likewise the latter limit signifies the quintessential potential, shown in figure 4b. Both the potentials end with their respective normalization constants asymptotically.

Thus, we finally obtain the required limiting potentials for inflation and quintessence, respectively, as

$$V_{\text{inf}}(\xi) = M^4 \left[1 - e^{-n} 2n\gamma \exp \left(-\sqrt{\frac{2}{3\alpha}} \frac{\xi}{M_P} \right) \right] \quad (2.17)$$

and

$$V_{\text{quint}}(\xi) = V_{\Lambda} \left[1 + e^n 2n\gamma \exp \left(\sqrt{\frac{2}{3\alpha}} \frac{\xi}{M_P} \right) \right]. \quad (2.18)$$

In figures 4a and 4b we have plotted these two potentials normalized by M^4 and V_{Λ} respectively, against ξ/M_P for $n = 2$, $\gamma = 0.4$ and $\alpha = 0.001, 0.005$ and 0.01 . $V_{\text{inf}}(\xi)$ reaches M^4 asymptotically in positive side of ξ and the $V_{\text{quint}}(\xi)$ dies down to V_{Λ} in the same way for the negative ξ -values.

Now, we shall proceed with the simplified version of quintessential α -attractor potential with EDE of Eq. (2.17) with the concept that ξ is sub-Planckian⁹ in entire field space, which is an essential requirement for the dynamical mode analysis, described in the next section¹⁰.

3 Quantum treatment of perturbation during inflation and associated parameters — a very brief overview

Now, we shall describe, in a nutshell, the theories applied for the quantum k -mode analysis to explore the aspects of EDE during inflation in parameter estimation process. This calculational framework has been developed in Ref. [169] for α -attractor and further elaborated in Ref. [168] in the context of quintessential α -attractor. The reader is referred to Refs. [168, 169] for details.

⁹that means non-canonically it remains always within the pole boundaries.

¹⁰We do not directly deal with the quintessential potential of Eq. (2.18), as the main work of the present paper is the microscopic mode analysis of the inflaton perturbation in k -space.

3.1 Quasi de-Sitter Hubble-exit of the dynamical inflaton modes and their evolutions

The primordial quantum nuggets are found to be nearly scale-invariant, non-Gaussian and adiabatic, which implies that all the components of the universe including the dark energy/quintessence have emerged from the undulations of one single scalar field - the inflaton field [205, 206]. In this process, the inflaton modes play the pivotal role. During the contraction of the Hubble sphere along with the exponential expansion of spacetime, they exit the horizon and become frozen. After these modes, encoded with the initial conditions, re-enter the causal sphere, they evolve as classical density perturbations [208].

The inherent uncertainties of the quantum modes ascribe a dynamical behaviour to the exiting mechanism, over a quasi de-Sitter metric background following $k = aH$ for the scale factor a and Hubble parameter H , which we term as *dynamical horizon exit* (DHE) [168]. This acts like a one-to-one mapping $\varphi : \mathbb{R} \rightarrow \mathbb{R}$ between t and k spaces as $k = \varphi(t) = a(t)H(t)$. We can consider the mapping φ as an operator $\hat{\varphi}$ in \mathbb{R} and then DHE implies a non-standard derivative identity

$$\hat{\varphi} (\ddot{a}^{-1} \partial_t) \equiv \partial_k \quad \text{for } k \in \mathbb{K} \subset \mathbb{R} \quad (3.1)$$

where \mathbb{K} is a subspace of all the *dynamical modes* crossing the horizon. This relation converts the temporal evolution of the inflaton field into its mode-dependent evolution in the inflationary metric space.

A particular statistical correlation always exists between two quantum nuggets over the expanding background, which carries the information about the specific initial condition buried inside the quantum fluctuations. It can be of scalar or tensor type depending upon the nature of perturbation in the metric. This correlation acts like a cosmic code of the present observable universe involving the CMBR through various parameters like power spectra, spectral indices and tensor-to-scalar ratio *etc.* We shall briefly describe them for the model concerned, in the next subsection.

Here, we follow the linear perturbative framework which is the simplest and the most effective way for decryption of CMB angular power spectra, as suggested by Planck data [7, 8]. Thus, we express the quantum mode function $\xi(t, k)$ as a linear combination of its zeroth order ($\xi^{(0)}(t)$) and first order ($\delta\xi(t, k)$) parts as

$$\xi(t, k) = \xi^{(0)}(t) + \delta\xi(t, k). \quad (3.2)$$

The dynamics of $\xi^{(0)}(t)$ and $\delta\xi(t, k)$ are dictated by their respective time domain evolution equations derived in Ref. [169] from Friedmann equations and continuity equation of Einstein's general theory of relativity.

Now, when we map the temporal dependencies of the evolution equations into the mode dependencies by the DHE condition $k = a(t)H(t)$ using the derivative transformation of Eq. (3.1), the modes become dynamical which cross the Hubble horizon at random times. This randomness is microscopically induced in the initial conditions, manifesting in the statistical correlations of the perturbations through mode-dependent power spectra and spectral indices. In order to measure these parameters precisely in momentum space, we need to solve a set of k -mode evolution equations of the inflaton field ($\xi^{(0)}(k)$) and its first order perturbation ($\delta\xi(k)$) over the fluctuating metric background, which is a certain gauge invariant combination of metric perturbation, called the Badeen potential [205]. Such equations have been derived in [169] using the DHE and the attributes for slow-roll inflation.

The perturbative evolution equations in k -space thus constitute a system of non-linearly coupled ordinary differential equations of three independent variables $\xi^{(0)}$, $\delta\xi$ and the Bardeen potential. But, according to the adiabaticity condition¹¹ [209, 210], only the self-consistent solution of $\delta\xi$ under appropriate boundary values will be utilised to monitor the mode responses of the cosmological parameters, described below.

3.2 Inflationary parameters for EMQA model

The statistical correlations of scalar and tensor perturbations connected with the quantum fluctuations as initial conditions are quantified by various cosmological parameters constrained by Planck [7, 8]. These parameters are dynamical and hence momentum dependent. In this section, we derive some of the required parameters for the potential considered in Eq. (2.17) using all the formulae mentioned in earlier works [168, 169].

The number of remaining e-folds of an inflaton mode (sometimes called, *scale*) at the moment of leaving the horizon is obtained as,

$$N(\xi) = \frac{3\alpha}{4n\gamma e^{-n}} \left[e^{\sqrt{\frac{2}{3\alpha}}\xi} - e^{\sqrt{\frac{2}{3\alpha}}\xi_{\text{end}}} \right] - \sqrt{\frac{3\alpha}{2}} (\xi - \xi_{\text{end}}) \quad (3.3)$$

where, the end-value of the scalar field,

$$\xi_{\text{end}} = \sqrt{\frac{3\alpha}{2}} \ln \left[\gamma e^{-n} \left(\frac{2n}{\sqrt{3\alpha}} + 2n \right) \right] \quad (3.4)$$

corresponds to unit value of the first potential slow-roll parameter. This is the point where the inflation ends. For a successful model building, this point should be as far as possible from the starting point¹² *i.e.* $\xi_{\text{end}} \ll \xi$. In fact, we can verify it by putting, for example, $n = 2$, $\alpha = 0.001$ and $\gamma = 0.4$ in Eq. (3.4) which yields $\xi_{\text{end}} = 0.055$, which is significantly small.

Putting the expression of ξ_{end} of Eq. (3.4) in Eq. (3.3) and keeping only the dominating exponential terms we obtain,

$$N(\xi) \approx \frac{3\alpha}{4n\gamma e^{-n}} \left[e^{\sqrt{\frac{2}{3\alpha}}\xi} - \gamma e^{-n} \left(\frac{2n}{\sqrt{3\alpha}} + 2n \right) \right]. \quad (3.5)$$

For $n \gg 1$ and $\gamma \ll 1$ (needed for EDE model building) we can further approximate $N(\xi)$ as,

$$N(\xi) \approx \frac{3\alpha}{4n\gamma e^{-n}} e^{\sqrt{\frac{2}{3\alpha}}\xi}. \quad (3.6)$$

Now, we can write the k -dependent number of remaining e-folds as

$$N(k) \approx \frac{3\alpha}{4n\gamma e^{-n}} e^{\sqrt{\frac{2}{3\alpha}}\xi(k)}. \quad (3.7)$$

¹¹The condition says that the amplitude of the adiabatic spectrum of the perturbation is characterized by co-moving curvature perturbation \mathcal{R} only. In spatially flat gauge, \mathcal{R} is measured in terms of the inflaton perturbation (which is $\delta\xi$, here) as $\mathcal{R} = H \frac{\delta\xi}{\dot{\xi}^{(0)}}$ [205]. Therefore, in our context, $\delta\xi$ is the only degree of freedom for calculating the cosmological parameters.

¹²This is actually an important requirement for large field model [205] *e.g.* slow-roll inflation, which is found to be effective in parameter estimation as per Planck data.

Here the factor γe^{-n} in the denominator is a new term, which was not present in the earlier model [168]. This term carries the signature of EDE. The expression of $N(k)$ in k -space will be exploited to fix the proper boundary values for solving the dynamical mode equations of perturbations.

A two-point correlation [205] is found to exist due to quantum fluctuations during inflation between two scalar perturbations of different momenta. All the crucial information regarding this correlation are encoded in a statistical measure, called the *scalar power spectrum* $\Delta_s(k)$. In the simplest version of linear cosmological perturbation the $\Delta_s(k)$ is Gaussian. Primordial non-Gaussianity [211] is found to be negligible in first order single field slow-roll perturbation [212, 213] and is significant mainly in higher order correlations like three-point correlation or *cosmic bispectrum* [214] and multi-field models [215]. Therefore, we do not attempt to compute higher order correlations and proceed with two-point correlation which is effectively Gaussian. In the present model, we get the $\Delta_s(k)$ in dimensionless format in terms of $N(k)$ using Eqs. (2.17) and (3.7) as,

$$\Delta_s(k) = \left(\frac{M^2}{3\pi\sqrt{2\alpha}} \right)^2 \left(\frac{\left(N(k) + \sqrt{\frac{3\alpha}{4}} \right)}{\left(N(k) + \sqrt{\frac{3\alpha}{4}} + \frac{3\alpha}{2} \right)^{1/3}} \right)^3. \quad (3.8)$$

Apart from probing the statistical information of primordial perturbations, the power spectra specifically $\Delta_s(k)$ has another crucial role to play. It actually determines the scale of inflation, M , through the amplitude of scalar perturbation $A_s(k)$ by the technique described in Ref. [168] with respect to a pivot scale k_* ¹³ for which $\Delta_s(k_*) = A_s(k_*)$. Following this method we obtain

$$M^4(A_s(k_*), N(k_*), \alpha) = 18\pi^2\alpha A_s(k_*) \left(N(k_*) + \sqrt{\frac{3\alpha}{4}} \right)^{-2} e^{\left(\frac{3\alpha}{2} \left(N(k_*) + \sqrt{\frac{3\alpha}{4}} \right)^{-1} \right)}. \quad (3.9)$$

This is widely known as the ‘*COBE/Planck normalization*’ for inflationary energy scale or the scale of inflaton potential.

¹³The order of this scale is actually same as that of the modes of the inflaton field, which indicates the range of k at which the horizon exit occurs. This aspect will be more clear in next section.

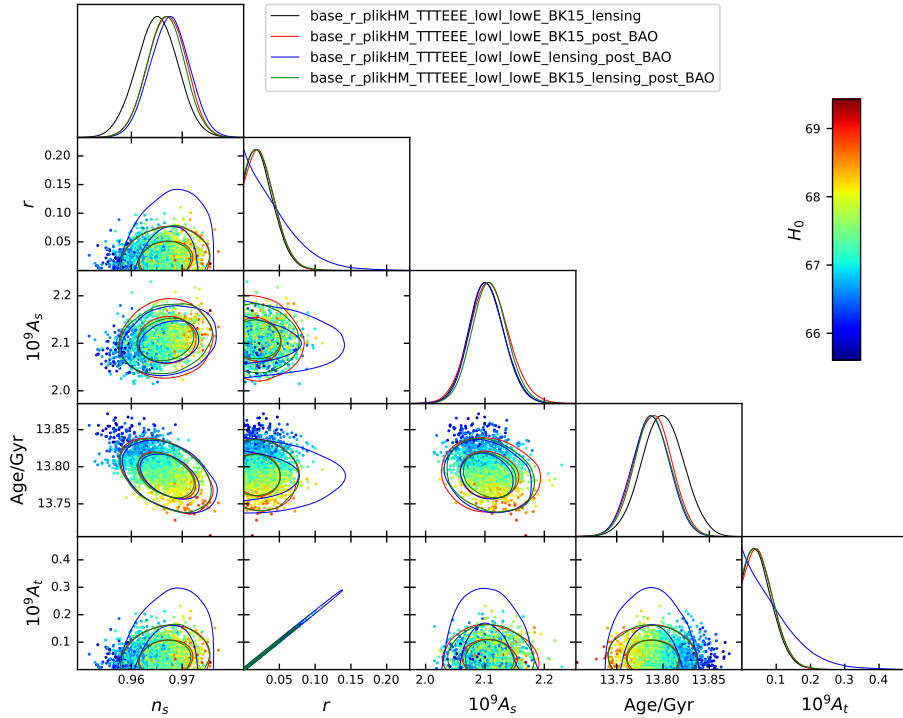


Figure 5. Planck constraints for various parameters to satisfy the present day Hubble parameter indicated in Eq. (1.1). This plot has been generated within GetDist (<https://getdist.readthedocs.io/en/latest/>) plotting utility by running the simulation data available in Planck Legacy Archive (<https://pla.esac.esa.int/>).

In the same way, the two-point correlation function for two mutually perpendicular tensor perturbations is determined by a dimensionless tensor power spectrum $\Delta_t(k)$. Using Eqs. (2.17) and (3.7) we get

$$\Delta_t(k) = \left(\sqrt{\frac{2}{3}} \frac{M^2}{\pi} \right)^2 \left(\frac{\frac{2N(k)}{3\alpha} + \sqrt{\frac{1}{3\alpha}}}{\frac{2N(k)}{3\alpha} + \sqrt{\frac{1}{3\alpha}} + 1} \right). \quad (3.10)$$

The first order logarithmic scale dependencies of scalar ($\Delta_s(k)$) and tensor ($\Delta_t(k)$) power spectra are determined by two spectral indices *viz.*, the scalar spectral index $n_s(k)$ and tensor spectral index $n_t(k)$ and the relative change of $\Delta_t(k)$ with respect to $\Delta_s(k)$ is given by the tensor-to-scalar ratio $r(k)$.

It is customary to measure the above-mentioned parameters in terms of number of remaining e-folds $N(k)$. Therefore, using Eqs. (2.17) and (3.7) for large $N(k)$ (so that $\mathcal{O}(\frac{1}{N^2}) \ll 1$) we obtain,

$$n_s(k) \approx 1 - \frac{2}{N(k)}, \quad (3.11)$$

$$n_t(k) \approx -\frac{3\alpha}{2N(k)^2} \quad (3.12)$$

and

$$r(k) \approx \frac{12\alpha}{N(k)^2}. \quad (3.13)$$

Eqs. (3.11)-(3.13) are of the same forms as those of the famous attractor equations of α -attractors, which are also identical to the predictions of quintessential α -attractors (see [168], [169]). The reason behind the latter resemblance is that all these models consist of the same type of non-canonical quadratic pole structures in kinetic parts of their respective Lagrangians. It is indeed a fundamental property of pole inflation that the cosmological predictions depend upon the nature of kinetic poles and are independent of the form and origin of the potential.

Now, Eq. (3.11) implies that $n_s \lesssim 1$, signifying that the primordial cosmological perturbation is *nearly scale invariant*. The tiny mode dependency can be measured in terms of its logarithmic derivatives of various orders. In linear perturbative formalism, it is sufficient to measure the first order one, which is called the running of spectral index $\alpha_s(k)$.

The rate of inflationary spacetime expansion in Friedmann universe is measured by the corresponding Hubble parameter $H_{\text{inf}}(k)$. Using Eqs. (2.17) and (3.7) $H_{\text{inf}}(k)$ can be expressed in terms of $N(k)$ as,

$$H_{\text{inf}}(k) = M^2 \sqrt{\frac{\frac{2N(k)}{\sqrt{3\alpha}} + 1}{\frac{6N(k)}{\sqrt{3\alpha}} + 3 + 3\sqrt{3\alpha}}}. \quad (3.14)$$

According to Planck-2018 [7, 8], in order to obtain the correct amount of scalar perturbation of amplitude $A_s(k_*) = 2.1 \pm 0.03 \times 10^{-9}$, tensor perturbation of amplitude $A_t(k_*)^{14} < 0.1 \times 10^{-9}$, present day vacuum density $V_\Lambda \sim 10^{-120} M_P^4$, scalar spectral index $n_s = 0.9649 \pm 0.0042$ with tensor-to-scalar ratio $r_{0.002} < 0.064$ (see figure 5¹⁵), running of spectral index $\alpha_s(k_*) = -0.0045 \pm 0.0067$ within 68% CL and the inflationary Hubble parameter $H_{\text{inf}}(k_*) < 6.07 \times 10^{13}$ GeV or $H_{\text{inf}}(k_*) < 2.5 \times 10^{-5}$ in reduced Planck unit within 95% CL at $k_* = 0.002 \text{ Mpc}^{-1}$ with $TT + TE + EE + \text{low}l + \text{low}E + \text{lensing} + \text{BAO}$, the scale of the inflaton potential should be $V_*^{1/4} = M < 6.99 \times 10^{-3}$ in reduced Planck unit or $M < 1.7 \times 10^{16}$ GeV. This requirement is equally important for satisfying the present day Hubble parameter $H_0^{\text{Planck}} = 67.44 \pm 0.58 \text{ Km s}^{-1} \text{ Mpc}^{-1}$ which determines that the current age of the universe is roughly 13.8 billion years.

In the next section, we shall continue our discussion regarding estimation of all necessary cosmological parameters described above in the context of the EMQA model. Our plan is first to make ready the model for calculations by fitting the inflationary and the quintessential energy scales with COBE/Planck normalisation condition derived in Eq. (3.9). Then, we numerically solve the dynamical mode equations of perturbations as in Refs. [168, 169] by Wolfram Mathematica 12.0, for the simplified inflaton potential of Eq. (2.17) under appropriate boundary conditions within a certain range of k -values. The results are then employed to compute and plot the required parameters using Eqs. (3.7), (3.8) and (3.10)-(3.14) within the same specified k -range for a set of predetermined model parameters. In this way, we explore the effects of EDE in parameter estimation process and thereby verify some of its interesting features. At the end, we shall make use of the Planck bounds to constrain the α factor, which is the primary motivation of the present work.

¹⁴The $A_t(k_*)$ is calculated by the empirical formula [205] $A_t(k_*) = \Delta_t(k) \left(\frac{k}{k_*}\right)^{-n_t(k_*)}$.

¹⁵Based on observations obtained with Planck (<http://www.esa.int/Planck>), an ESA science mission with instruments and contributions directly funded by ESA Member States, NASA, and Canada.

4 Results and discussions

4.1 Prerequisites

1. In the present formalism, the mechanism underlying inflation is the ‘*dynamical horizon crossing*’ of cosmological scales or the inflaton modes. Now, which mode (of momentum k) will exit first, depends upon the corresponding number of remaining e-folds $N(k)$. This means that those modes will cross the horizon first for which the number of remaining e-folds is maximum, which is roughly 60 e-folds as required by Planck observations. The order of these modes/scales can be estimated by that of the pivot scale k_* which is around 0.002 Mpc^{-1} . This is the reference scale with respect to which Planck constrains the cosmological parameters. Therefore we can expect that the exiting modes should be of the order of 10^{-3} Mpc^{-1} .

Motivated by these ideas we select $N = 63.49$ ¹⁶ as the starting point of dynamical crossing of quantum modes. We also choose the same initial conditions as considered in Refs [168, 169]. The outputs are then allowed to plot in the k -range $0.001 - 0.009 \text{ Mpc}^{-1}$. We assume, here, that all the required conditions for the selection of Bunch-Davies vacuum state [216–219] during DHE are fulfilled, as the self-consistency for the solutions of the mode equations is concerned.

2. In Ref. [168], it was shown that $0.1 \leq \alpha \leq 4.3$ is a valid range for α in quintessential α -attractor model to explain both the inflationary and the DE expansions successfully. A recent study [113] on non-oscillating EDE model of α -attractor reveals that the parameter α should be $\sim 10^{-3}$ in order to solve the H_0 -tension. Therefore, in the present analysis we consider three hierarchies of α -values. In the low end of range we choose $\alpha = 0.001, 0.005, 0.010$, in the mid range $\alpha = 0.05, 0.10, 0.50$ and in high end of range $\alpha = 1.0, 2.5, 4.3$.
3. We determine the amplitudes of power spectra through COBE/Planck normalisation condition of Eq. (3.9) and the nine value of α described earlier by evaluating the factor M with the considerations $N(k_*) = 63.49$ and $A_s(k_*) = 2.1 \times 10^{-9}$ as enlisted in table 1. All the M values are less than M^{Planck} and therefore conform to the Planck requirements.

Table 1. COBE/Planck normalised M for nine values of α with $M_P = 2.43 \times 10^{18} \text{ GeV}$.

α	$M(M_P)$	$M \text{ (GeV)}$	$M^{\text{Planck}}(M_P)$	$M^{\text{Planck}} \text{ (GeV)}$
0.001	5.58×10^{-4}	1.35×10^{15}	6.99×10^{-3}	1.70×10^{16}
0.005	8.35×10^{-4}	2.03×10^{15}		
0.010	9.92×10^{-4}	2.41×10^{15}		
0.050	1.48×10^{-3}	3.60×10^{15}		
0.100	1.76×10^{-3}	4.28×10^{15}		
0.500	2.64×10^{-3}	6.41×10^{15}		
1.000	3.14×10^{-3}	7.63×10^{15}		
2.500	3.96×10^{-3}	9.62×10^{15}		
4.300	4.57×10^{-3}	1.11×10^{16}		

¹⁶which is the same value as taken in the quintessential model [168].

4. The other model parameters *viz.*, γ and n are picked up on the basis of the model requirements for EDE mentioned in Section 2. We choose a small fractional value of γ , $\gamma = 0.0818$ and a little large value of n , $n = 8$. With this choice of the parameter space, the responses of the simplified potentials for inflation of Eq. (2.17) and for quintessence of Eq. (2.18) are represented in figures 6a and 6b, respectively, for the first family of α -values.

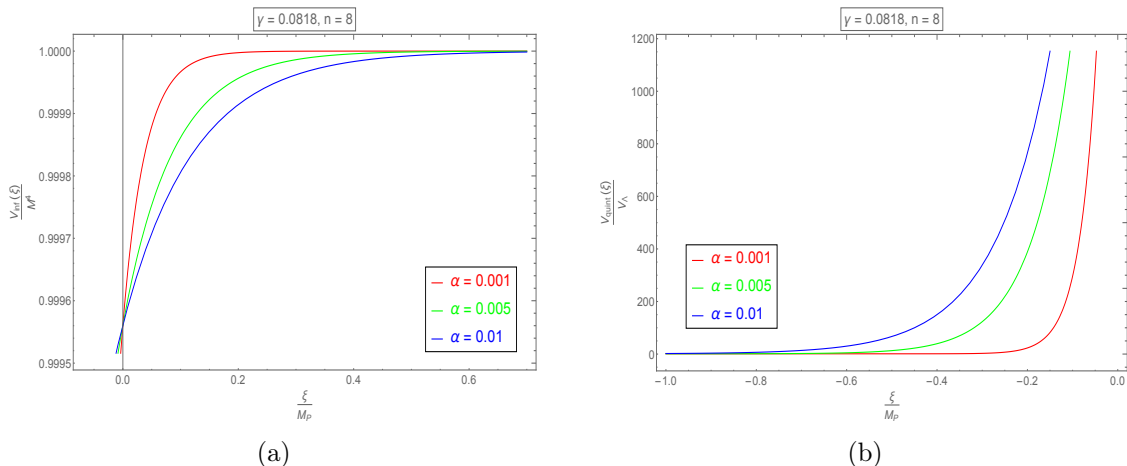


Figure 6. Inflation and quintessential potentials for $\gamma = 0.0818$, $n = 8$ and three values of α .

5. The choice of the parameter space would be satisfactory if the corresponding vacuum density matches with that of the Planck bound. Therefore, let us calculate the amplitude of the quintessential potential of Eq. (2.18) *i.e.* the present vacuum density V_Λ using the constraints discussed above. We first use the expression of V_Λ defined in Eq. (2.16),

$$V_\Lambda = \exp[-2\gamma \sinh(n)]M^4 = 10^{-u} \quad (\text{say}). \quad (4.1)$$

Then

$$u = \frac{2\gamma \sinh(n) - 4 \ln M}{\ln 10}, \quad (4.2)$$

where M is the COBE/Planck normalisation constant measured in M_P unit and V_Λ is obtained in M_P^4 unit. Now, we convert V_Λ into a new expression given in [113] in presence of EDE

$$V_\Lambda^{\text{exact}} = \left(\frac{H_0^{\text{Planck}}}{H_0^{\text{SN}}} \right)^2 V_\Lambda = 0.8525 V_\Lambda \quad (4.3)$$

or, $10^{-v} = 0.8525 \times 10^{-u}$ (say).

Here, H_0^{Planck} and H_0^{SN} are the two values of the Hubble parameters from Planck and supernovae measurements, given in Eqs. (1.1) and (1.2) respectively. Ref. [113] shows that, this modified form of V_Λ is suitable for solving the Hubble tension. In this way, we encode the aspects of resolution of H_0 tension by EDE in the chosen set of parameters for the model, discussed in this paper.

Eq. (4.3) gives

$$v = u - \frac{\ln 0.8525}{\ln 10}. \quad (4.4)$$

Putting the expression of u from Eq. (4.2) in Eq. (4.4) we get,

$$v = \frac{2\gamma \sinh(n) - 4 \ln M}{\ln 10} - \frac{\ln 0.8525}{\ln 10} = \frac{2\gamma \sinh(n) - 4 \ln M - \ln 0.8525}{\ln 10}. \quad (4.5)$$

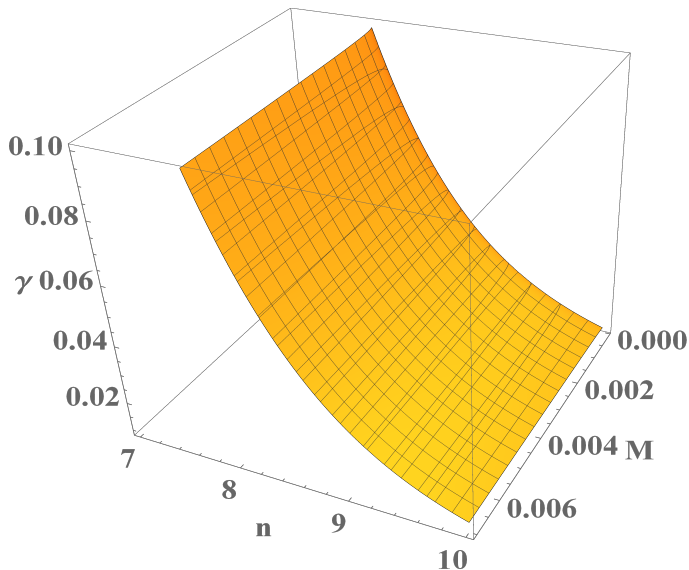


Figure 7. Three dimensional contour plot of n , γ and M for $v = 120$ according to Eq. (4.5). The figure shows that γ and n should belong in the closed intervals $[0.01, 0.09]$ and $[8, 10]$ respectively in order to have the M values within the COBE/Planck limit $M < 6.99 \times 10^{-3} M_P$ and vacuum density $V_\Lambda \sim 10^{-120} M_P^4$.

The order of the vacuum density, v , depends on the model parameters, n , γ and M . It also depends on α through M according to Eq. (3.9). If this order matches with the experimental value, then the model parameters automatically conform to the potential suitable for inflation, quintessence and EDE. Figure 7 shows the necessary ranges of model parameters in order to obtain the experimentally favoured value of vacuum density *i.e.* $V_\Lambda \sim 10^{-120} M_P^4$. Our chosen parameter space described by $n = 8$ and $\gamma = 0.0818$ lies within these ranges, so we can fairly expect that it will give satisfactory amount of vacuum density.

Now, using Eq. (4.5) the calculated values of the present-day vacuum density for considered values of α in the EDE-influenced quintessential α -attractor model are given in table 2.

Table 2. The EDE-modified values of V_Λ in the present model.

n	γ	α	$M(M_P)$	v	$V_\Lambda^{\text{exact}}(M_P^4)$	$V_\Lambda^{\text{Planck}}(M_P^4)$
8	0.0818	0.001	5.58×10^{-4}	118.982	1.042×10^{-119}	10^{-120}
		0.005	8.35×10^{-4}	118.282	5.224×10^{-119}	
		0.010	9.92×10^{-4}	117.983	1.039×10^{-118}	
		0.050	1.48×10^{-3}	117.288	5.152×10^{-118}	
		0.100	1.76×10^{-3}	116.987	1.030×10^{-117}	
		0.500	2.64×10^{-3}	116.281	5.240×10^{-117}	
		1.000	3.14×10^{-3}	115.981	1.045×10^{-116}	
		2.500	3.96×10^{-3}	115.578	2.642×10^{-116}	
4.300	4.57×10^{-3}	115.329	4.688×10^{-116}			

Tables 1 and 2 clearly show that the M and V_Λ for the chosen values of model parameters n , γ , α are in excellent agreement with Planck data.

In the above, we have set all the prerequisites and can proceed to analyse the solutions of the dynamical mode equations and estimate the cosmological parameters within the model constraints.

4.2 Inflaton field and its first order perturbation

In figures 8 and 9 we show the solutions of the inflaton field $\xi^{(0)}(k)$ and its first order perturbation $\delta\xi(k)$ for $\alpha = 0.001 - 4.3$ within $k = 0.001 - 0.009 \text{ Mpc}^{-1}$. The values of $\xi^{(0)}(k)$ are positive ranging from 0.072 to 0.1136 from $\alpha = 0.001$ to $\alpha = 0.01$ and afterwards it become negative from $\alpha = 0.05$ to $\alpha = 4.3$. The corresponding $\delta\xi(k)$ values range from 0.0005 to 0.004 in the entire range of α . The negative values of ξ beyond $\alpha = 0.01$ (*i.e.* $0.05 \leq \alpha \leq 4.3$) seem to be inconsistent. It should be positive for quintessential model of inflation since in that case the inflationary plateau remains at positive values of ξ . Actually there is a deep connection lying behind this odd behaviour with the EDE scenario and it necessitates further constraining of the parameter α . We shall explain this crucial aspect in detail in subsection 4.4.

So far as the values of $\delta\xi(k)$ are concerned, they are roughly 10 – 100 times smaller than $\xi^{(0)}(k)$ ¹⁷. Therefore it confirms that the linear perturbative framework is equally consistent in k -space as in t -space. Actually the k -space formulation appears to be an alternative to the usual formulation in time domain (see [113] for example), especially when the mode responses and estimations of the cosmological parameters are required during inflation. It is indeed a great advantage. However it has some limitations also. It can not be extended to post inflationary regime. Therefore all the ideas of reheating, preheating and particle production are outside the scope of the present framework.

Now, the solutions of $\xi^{(0)}(k)$ and $\delta\xi(k)$ can be suitably coupled to the inflaton potential in momentum space as

$$V(\xi(k)) = V(\xi^{(0)}(k)) + \partial_{\xi^{(0)}(k)} V(\xi^{(0)}(k)) \delta\xi(k) = V^{(0)}(k) + \delta V(k). \quad (4.6)$$

In this way, the quantum aspects of the inflaton perturbation are transferred microscopically into the potential in k -space. Therefore it is quite expected that the perturbative framework should work well with respect to the potential and its perturbation part also. That is exactly

¹⁷which can be easily realised by computing the ratio $\frac{\delta\xi(k)}{|\xi^{(0)}(k)|}$ at a particular k value.

what we observe in figures 10 and 11. The $V^{(0)}(k)$ s are found in the range $9.723 \times 10^{-14} - 3.93 \times 10^{-10}$ and the corresponding $\delta V(k)$ s from 3×10^{-20} to 8×10^{-14} . That is, δV is about $10^4 - 10^6$ times smaller than $V^{(0)}$. It is also quite clear that the orders of all $V^{(0)}(k)$ values are consistent with the COBE/Planck normalisation of Eq. (3.9) (see also table 1) which is very important for the parameter estimation, specifically the power spectra.

4.3 Mode responses of the parameters during EMQA-inflation

Figures 12 and 13 represent the COBE/Planck normalised scalar ($\Delta_s(k)$) and tensor ($\Delta_t(k)$) power spectra calculated from Eqs. (3.8) and (3.10) respectively. As α increases from $\alpha = 0.001$ to $\alpha = 4.3$, the $\Delta_s(k)$ remains almost unaltered up to $\alpha = 0.01$ and afterwards it decreases slowly, while $\Delta_t(k)$ increases monotonically at a particular value of k . The orders of $\Delta_s(k)$ is 10^{-9} and that for $\Delta_t(k)$ varies between $10^{-15} - 10^{-11}$. These values lie within the Planck bounds (see figure 5) which are consistent with the present day value of the Hubble parameter. The scalar and tensor tiny correlations are the seeds for today's observed large scale structures which are embedded in the initial conditions during inflation. Their imprints are found in the secondary anisotropies of CMB B -mode polarisation (which is very feeble and therefore hard to detect) and the density profile of stellar or galactic distribution (which is measured by gravitational lensing method).

The number of remaining e-folds $N(k)$ is plotted according to Eq. (3.7) in figure 14. $N(k)$ varies between $61.5 - 63.5$ for a given value of α , while at a fixed value of k it remains almost constant. At small values of k the number of remaining e-folds is approximately 63.5 and as k increases $N(k)$ decreases to around 61.5 . Such mode behaviour of $N(k)$ simulates the DHE scenario described in Section 3, according to which small modes exit at the beginning and high modes exit at the end of Hubble sphere contraction.

We shall now discuss about the spectral indices *i.e.* the scalar spectral index $n_s(k)$, tensor spectral index $n_t(k)$ and tensor-to-scalar ratio $r(k)$ which are related to the momentum dependencies of the power spectra $\Delta_s(k)$ and $\Delta_t(k)$ and their relative variations. For pole inflation (as in the present case), they obey simple expressions called the *attractor equations* which are dependent on the number of e-folds. We derived such equations (Eqs. (3.11)-(3.13)) in Section 3. These equations show that n_s is independent of α while $|n_t|$ and r are directly proportional to α . In figure 14 we have seen that $N(k)$ remains within $61.5 - 63.5$, irrespective of α . Thus it can be anticipated that $n_s(k)$ should follow the same pattern as that of $N(k)$, while $|n_t(k)|$ and $r(k)$ should increase with α . Figures 15, 16 and 17 demonstrate these facts, as expected. Now, the reason behind the monotonic increment of $r(k)$ with k for a specific value of α lies in the k -space behaviour of the two power spectra. At a particular value of α , the scalar power spectrum decreases with faster rate than that of tensor power spectrum. As a result, their ratio *i.e.* $r(k)$ increases with k . All the values of $n_s(k)$ ($0.9685 - 0.9674$), $n_t(k)$ ($(-3.95 \times 10^{-7}) - (-1.72 \times 10^{-3})$) and $r(k)$ ($3.15 \times 10^{-6} - 1.28 \times 10^{-2}$) satisfy the Planck constraints (see figure 5) quite well. Detecting such small orders of $r(k)$ ($\lesssim 10^{-3}$) is the target of many ongoing and forthcoming B -mode surveys [220].

The little scale dependency of $n_s(k)$ is usually visualized by the running of spectral index $\alpha_s(k)$ which we demonstrate by the figure 18. $\alpha_s(k)$ varies from $(-0.00040) - (-0.00060)$ for all values of α in the entire k range which match Planck data satisfactorily. The negative sign signifies the decreasing mode behaviour and the small values indicate approximate scale invariance of $n_s(k)$ with k .

Let us end our numerical and graphical analysis part by showing the inflationary Hubble parameter $H_{\text{inf}}(k)$ in figure 19 according to Eq. (3.14). The calculated values are in the range,

$1.8 \times 10^{-7} - 1.14 \times 10^{-5}$, which are supported by Planck data (see section 3). The orders of the $H_{\text{inf}}(k)$ values suggest that the inflation takes place in GUT scale ($\sim 10^{15}$ GeV).

In the course of dynamical mode analysis, we find that the obtained results for all the mode-dependent cosmological parameters are within the allowed ranges of Planck-2018 and do not deviate significantly. In fact, the graphical results also show that the cosmological parameters in quintessential EDE model are not very different in comparison to those in the model without EDE [168], specifically for $\alpha \geq 0.1$. Thus, we have verified a characteristic property of EDE, that, it does not considerably affect the parameters of the Λ CDM model. However it can have influence on V_Λ (see table 2) and also on α , as discussed in the next subsection.

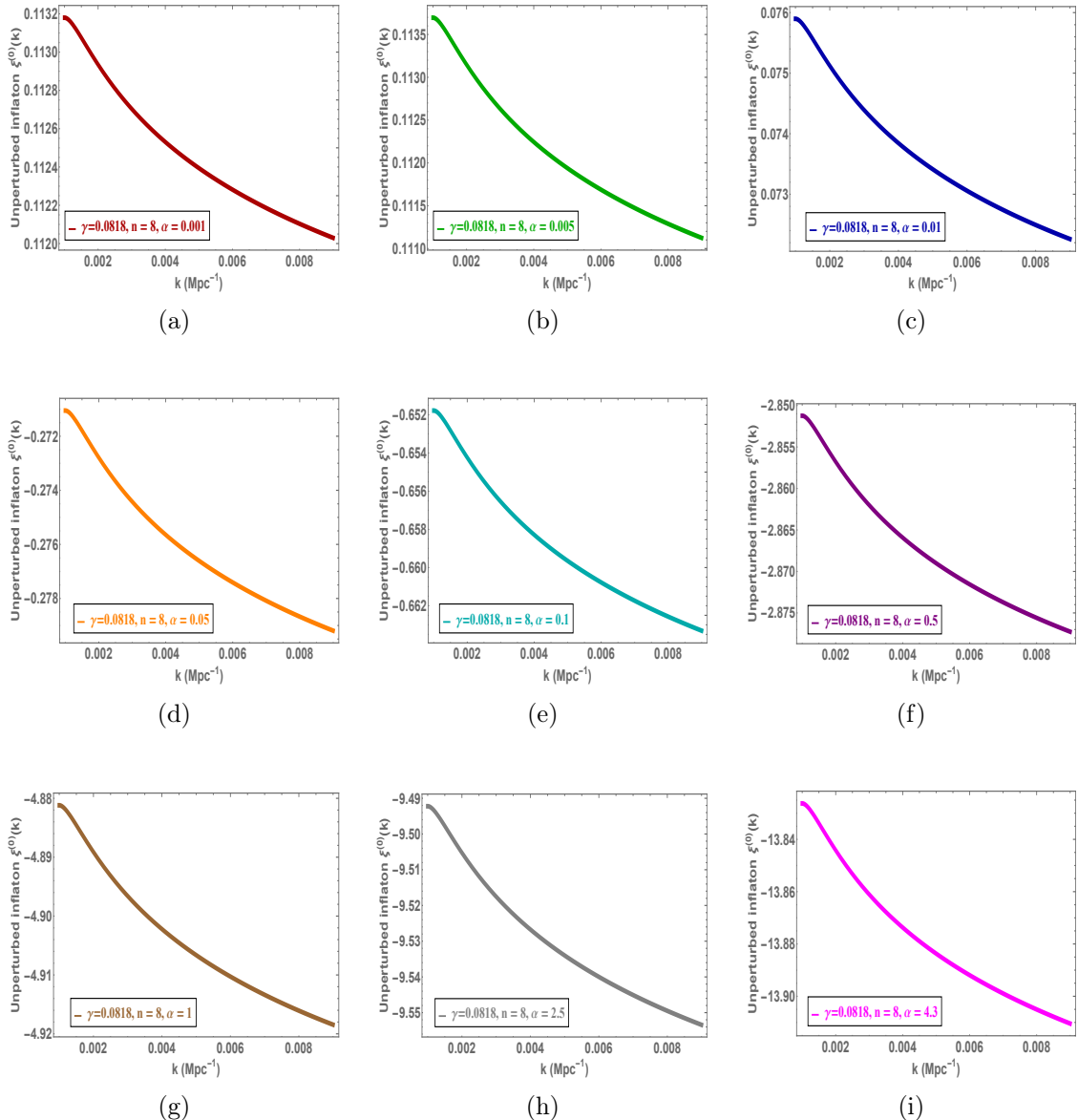


Figure 8. Zeroth order parts of the inflaton field $\xi(k)$ for nine values of α for $\gamma = 0.0818$ and $n = 8$. The values of $\xi^{(0)}(k)$ become increasingly negative from $\alpha = 0.05$ at a particular k value.

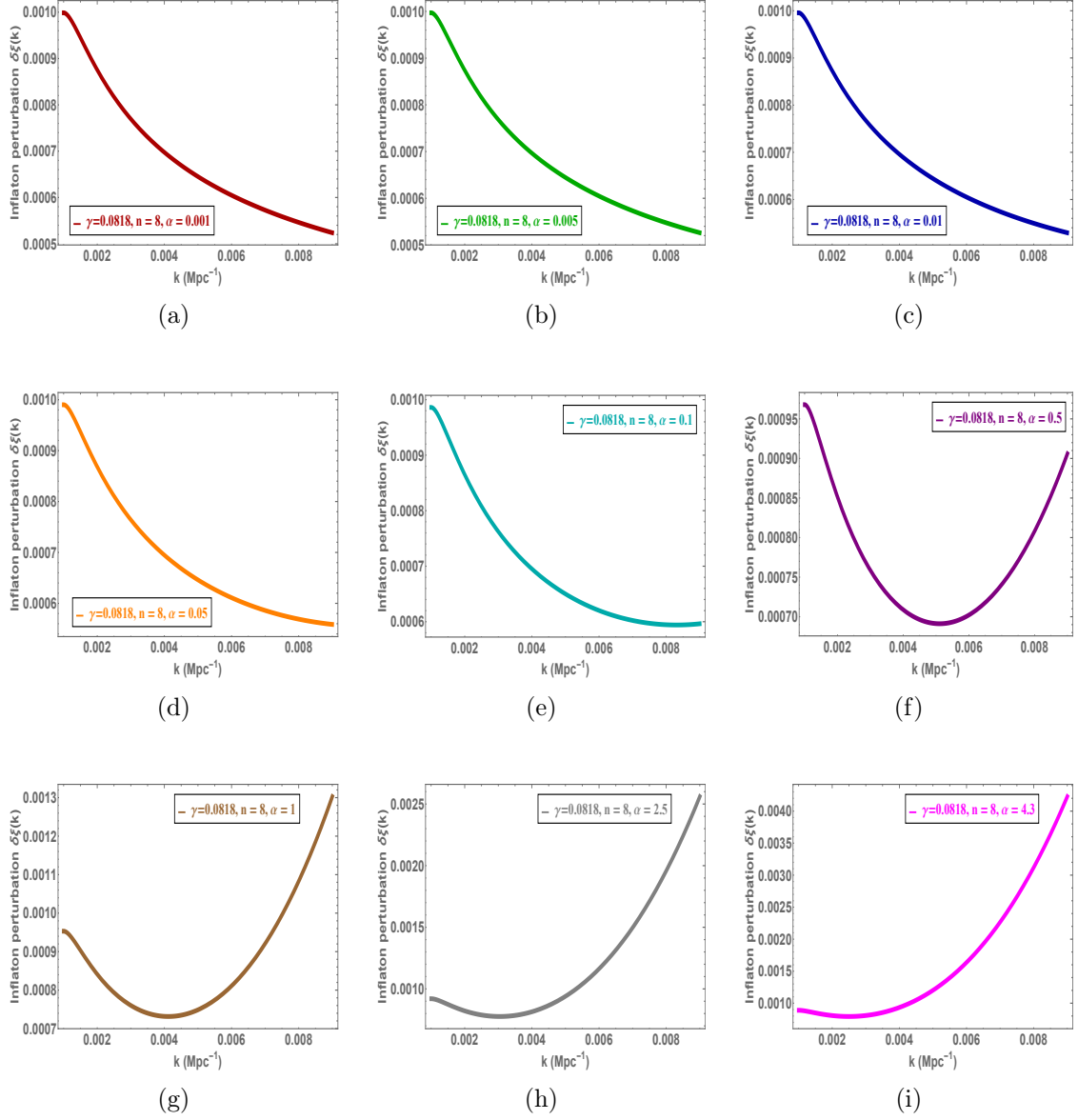


Figure 9. First order perturbed parts of the inflaton field for nine values of α for $\gamma = 0.0818$ and $n = 8$. Up to $\alpha = 0.1$ the $\delta\xi(k)$ is almost insensitive to α . After that, it tends to increase with the increase in α at a particular k -value. For $\alpha \geq 0.1$ the perturbation becomes stronger for $k \geq 0.005 \text{ Mpc}^{-1}$ than $k < 0.005 \text{ Mpc}^{-1}$.

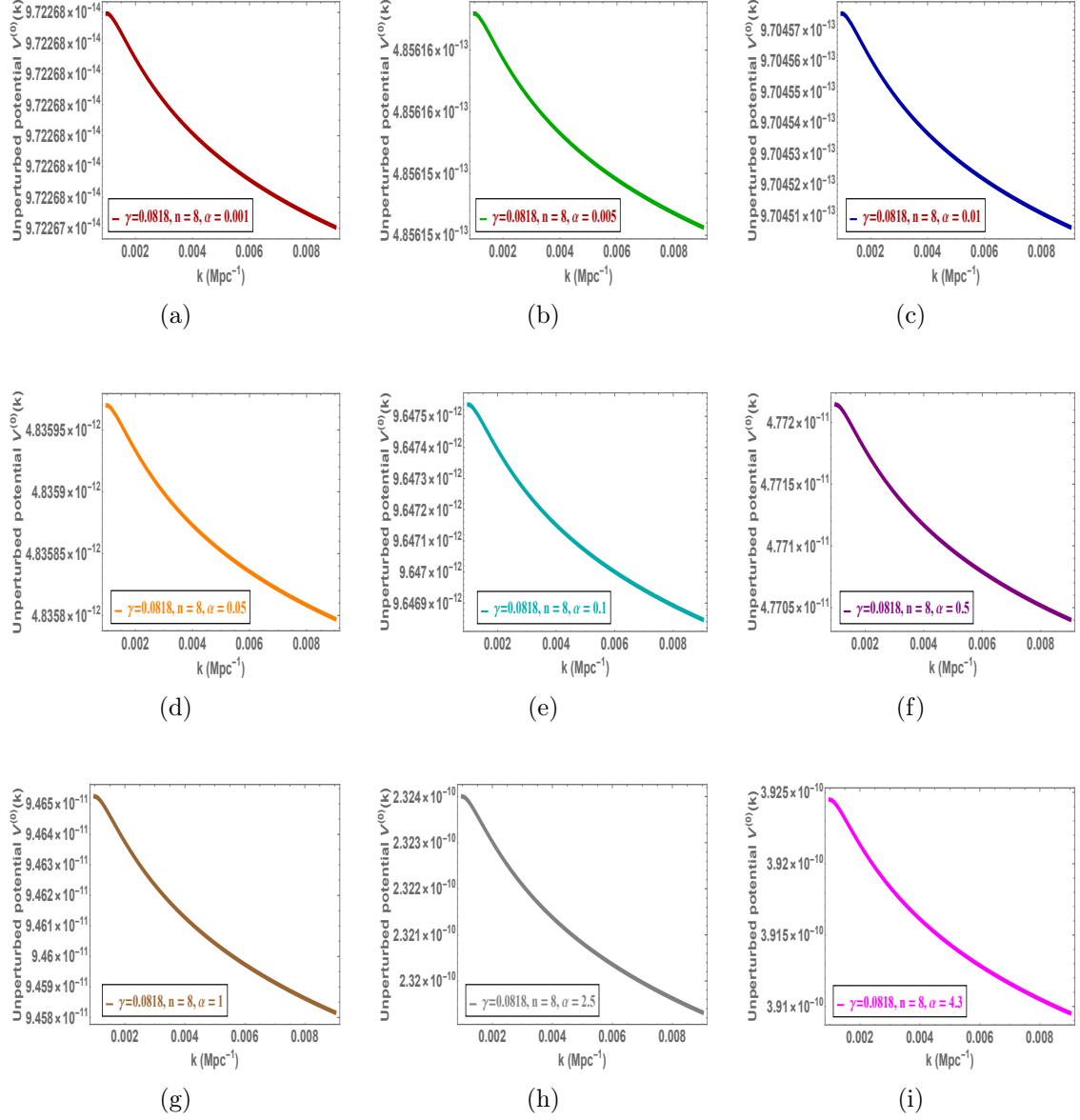


Figure 10. Zeroth order parts of the potential of Eq. (2.17) for nine values of α for $\gamma = 0.0818$ and $n = 8$. The values of $V^{(0)}(k)$ tend to increase with the increase in α at a particular k value.

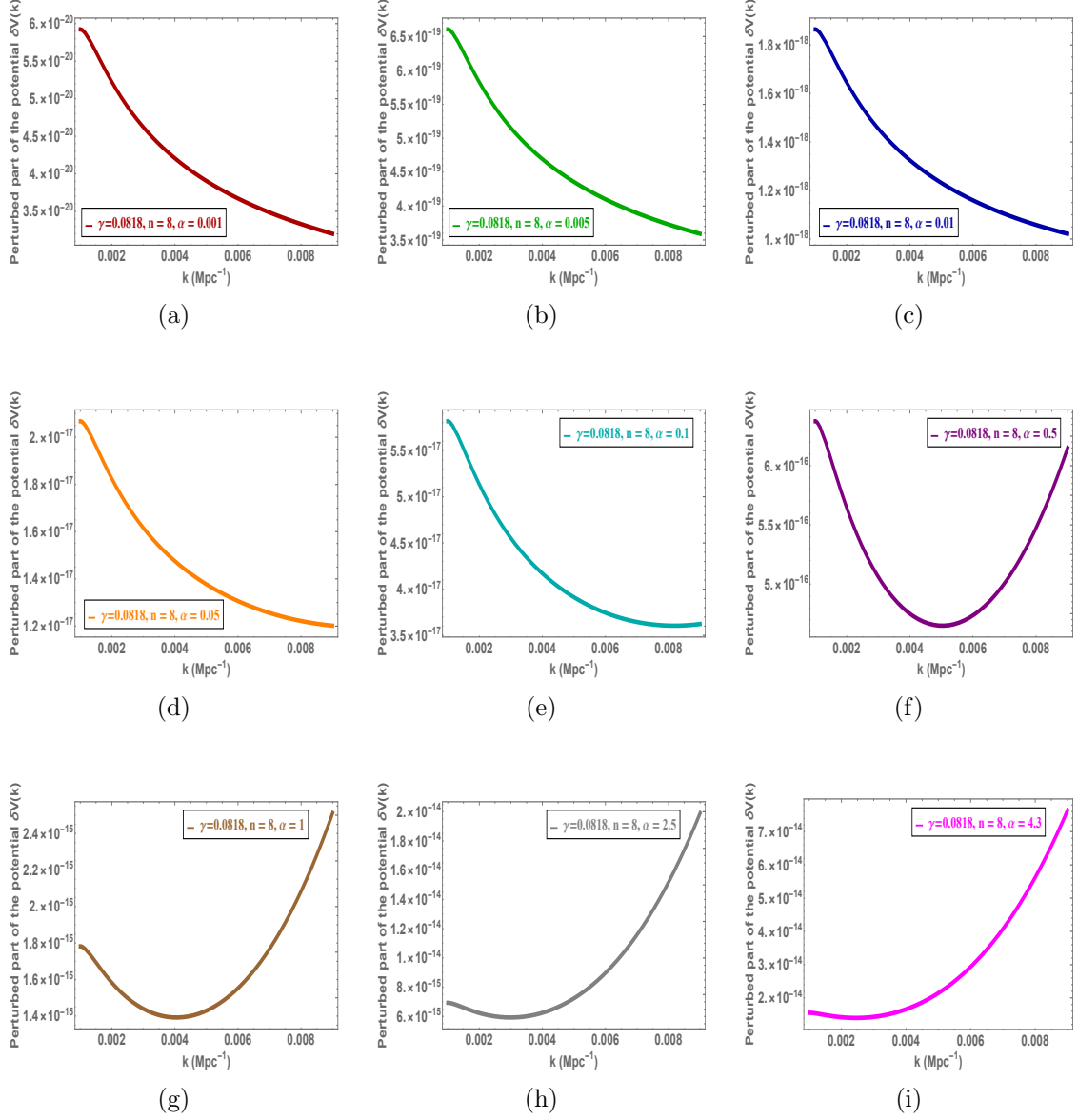


Figure 11. First order perturbed parts of the potential of Eq. (2.17) for nine values of α for $\gamma = 0.0818$ and $n = 8$. The values of $\delta V(k)$ tend to increase with the increase in α at a particular k -value. After $\alpha = 0.1$ the perturbation becomes stronger for $k \geq 0.005 \text{ Mpc}^{-1}$ than $k < 0.005 \text{ Mpc}^{-1}$.

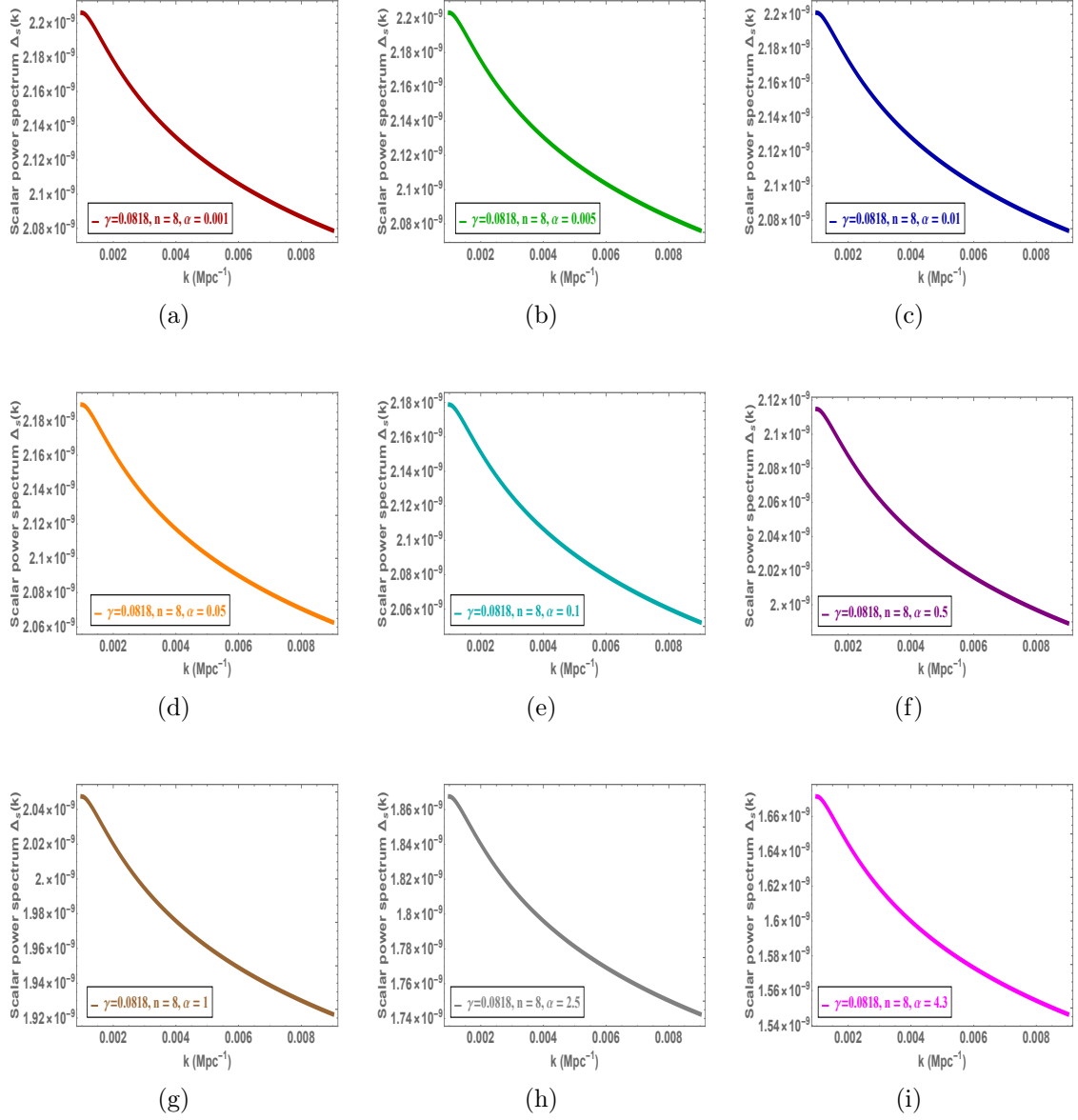


Figure 12. Scalar power spectra for nine values of α for $\gamma = 0.0818$ and $n = 8$. Up to $\alpha = 0.01$ the $\Delta_s(k)$ is almost insensitive to α and then it tends to decrease slowly with the increase in α at a particular k value.

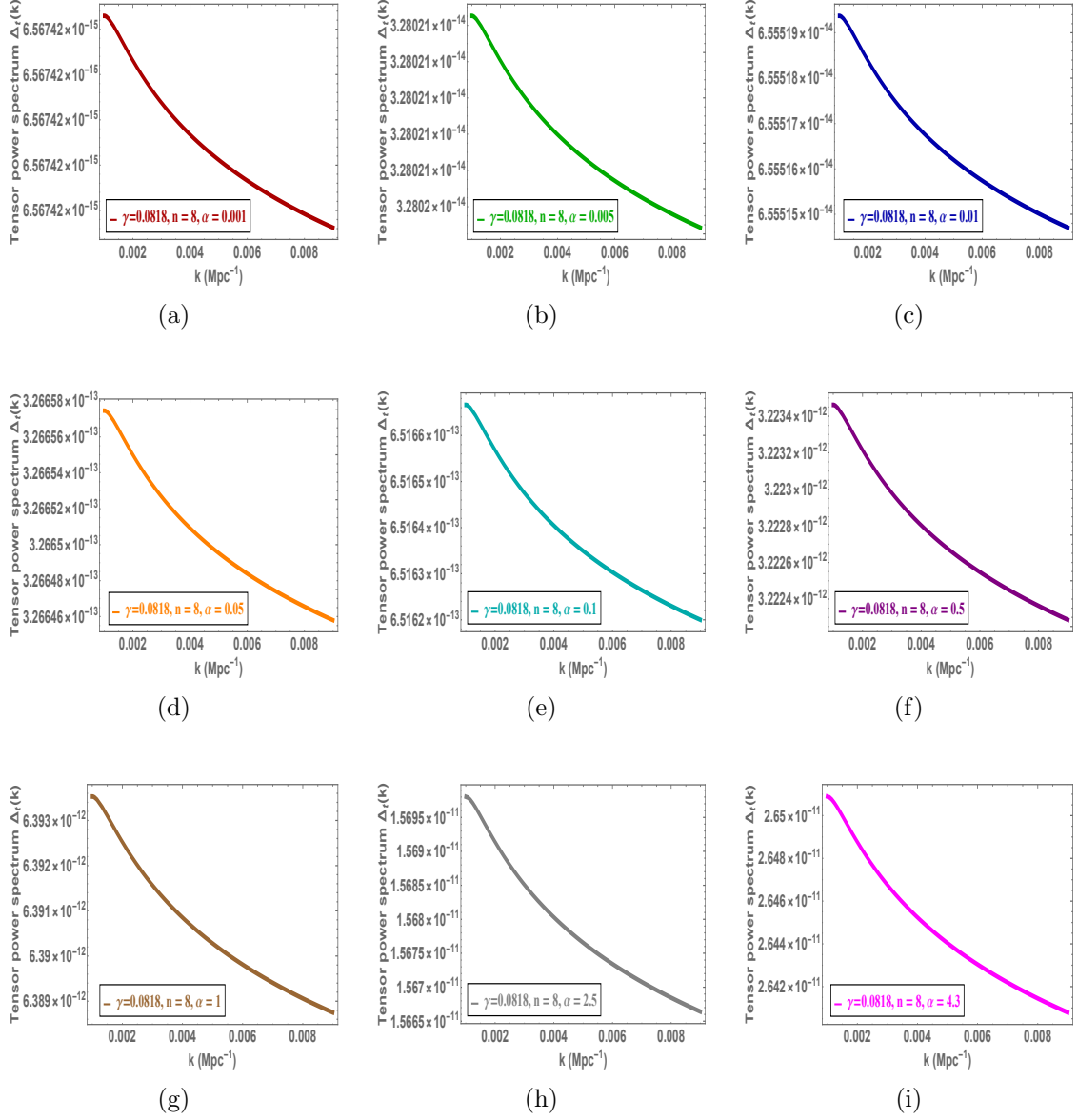


Figure 13. Tensor power spectra for nine values of α for $\gamma = 0.0818$ and $n = 8$. The values of $\Delta_t(k)$ tend to increase with the increase in α at a particular k value.

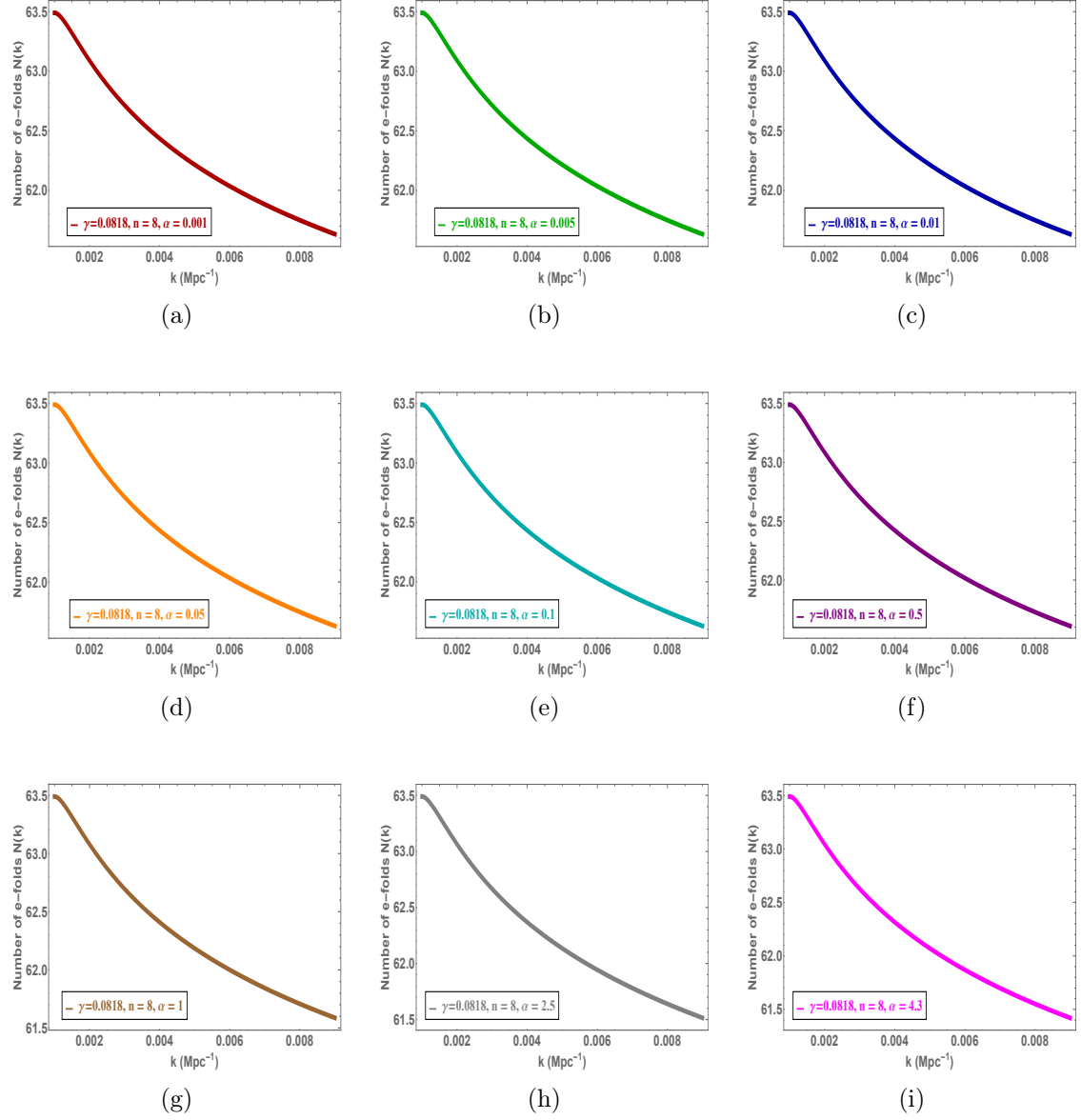


Figure 14. Number of remaining e-folds for nine values of α for $\gamma = 0.0818$ and $n = 8$. The values of $N(k)$ tend to remain same for all values of α .

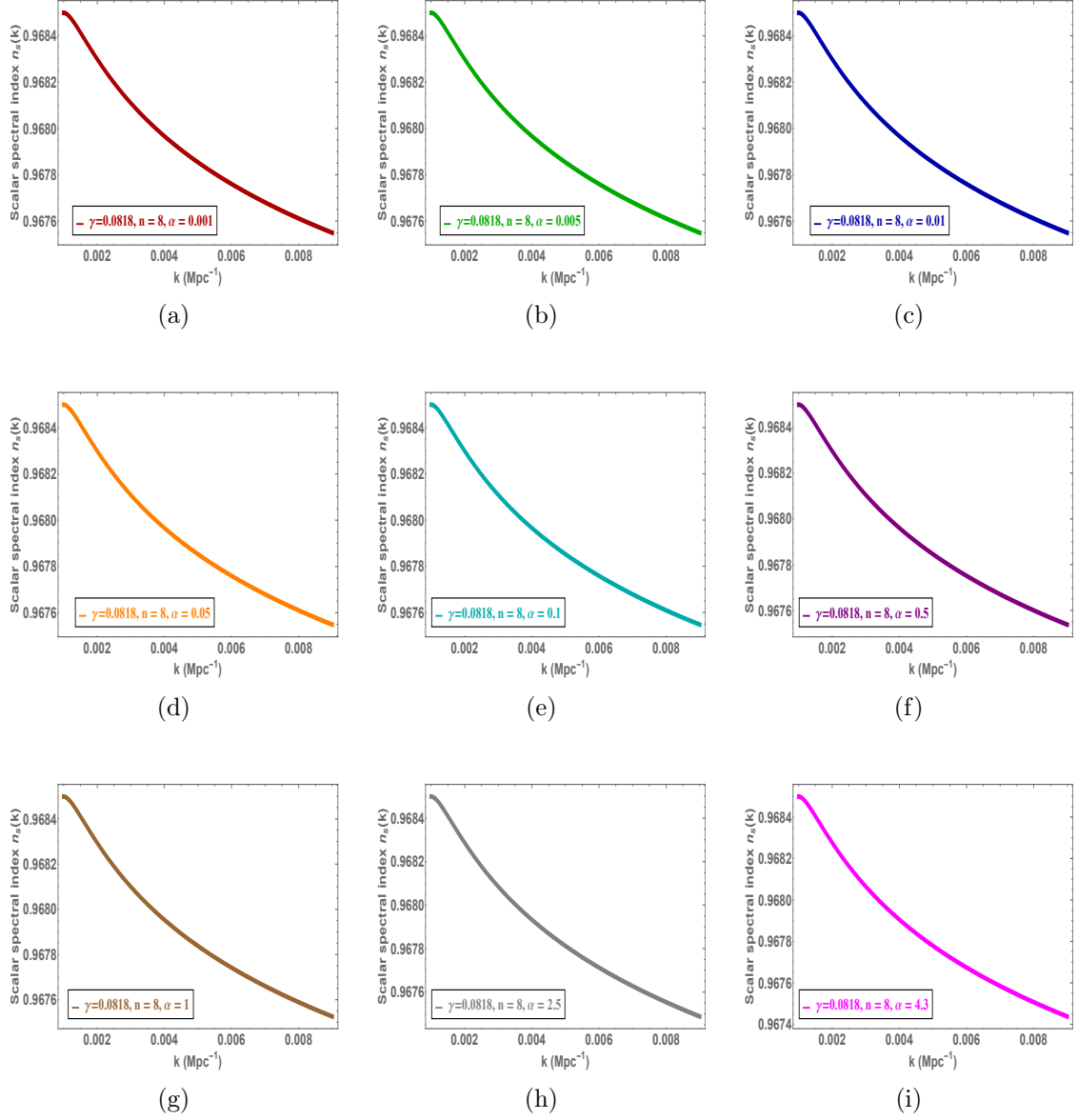


Figure 15. Scalar spectral indices for nine values of α for $\gamma = 0.0818$ and $n = 8$. The values of $n_s(k)$ tend to remain same for all values of α .

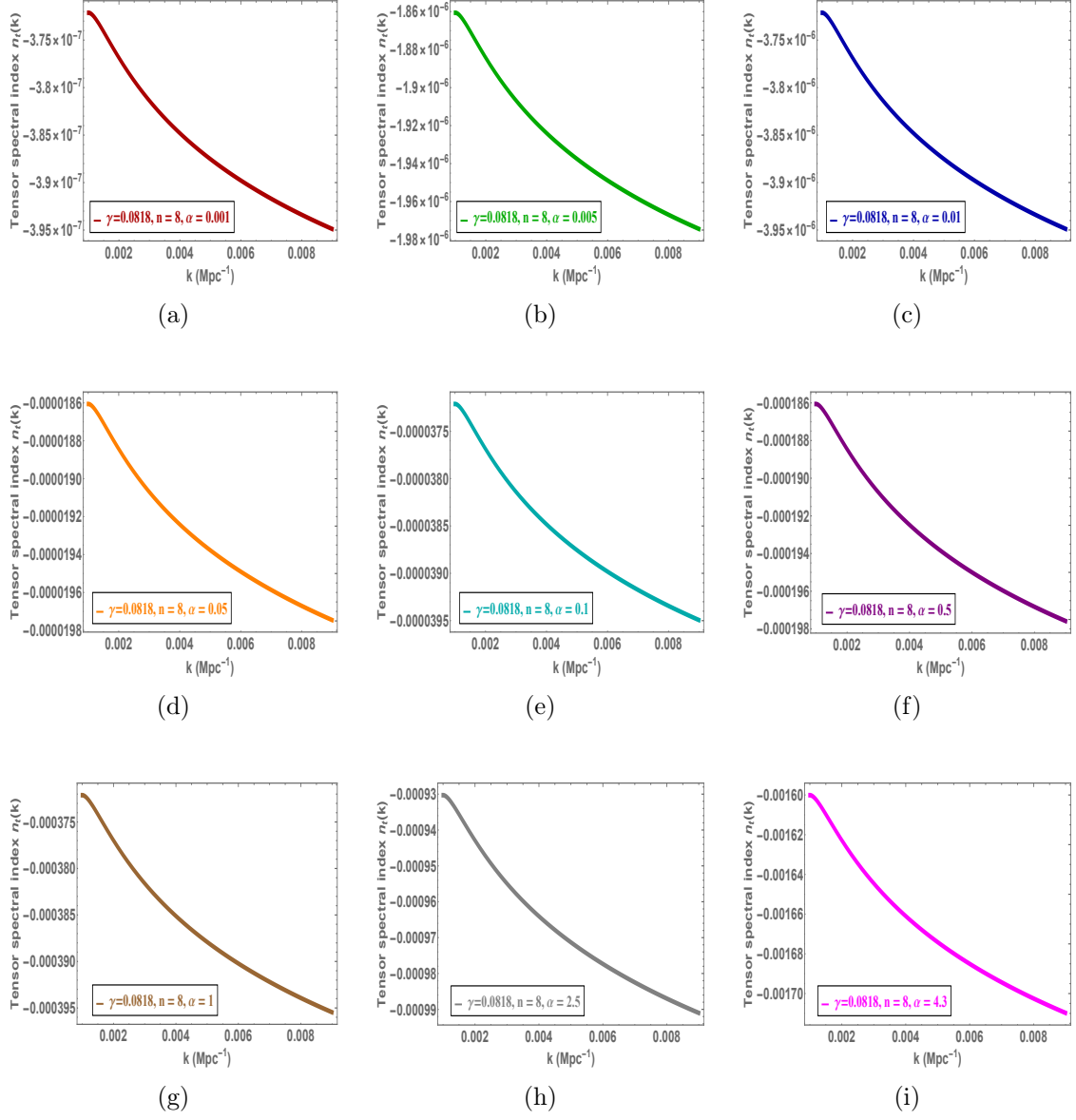


Figure 16. Tensor spectral indices for nine values of α for $\gamma = 0.0818$ and $n = 8$. The values of $|n_t(k)|$ tend to increase with the increase in α at a particular k value.

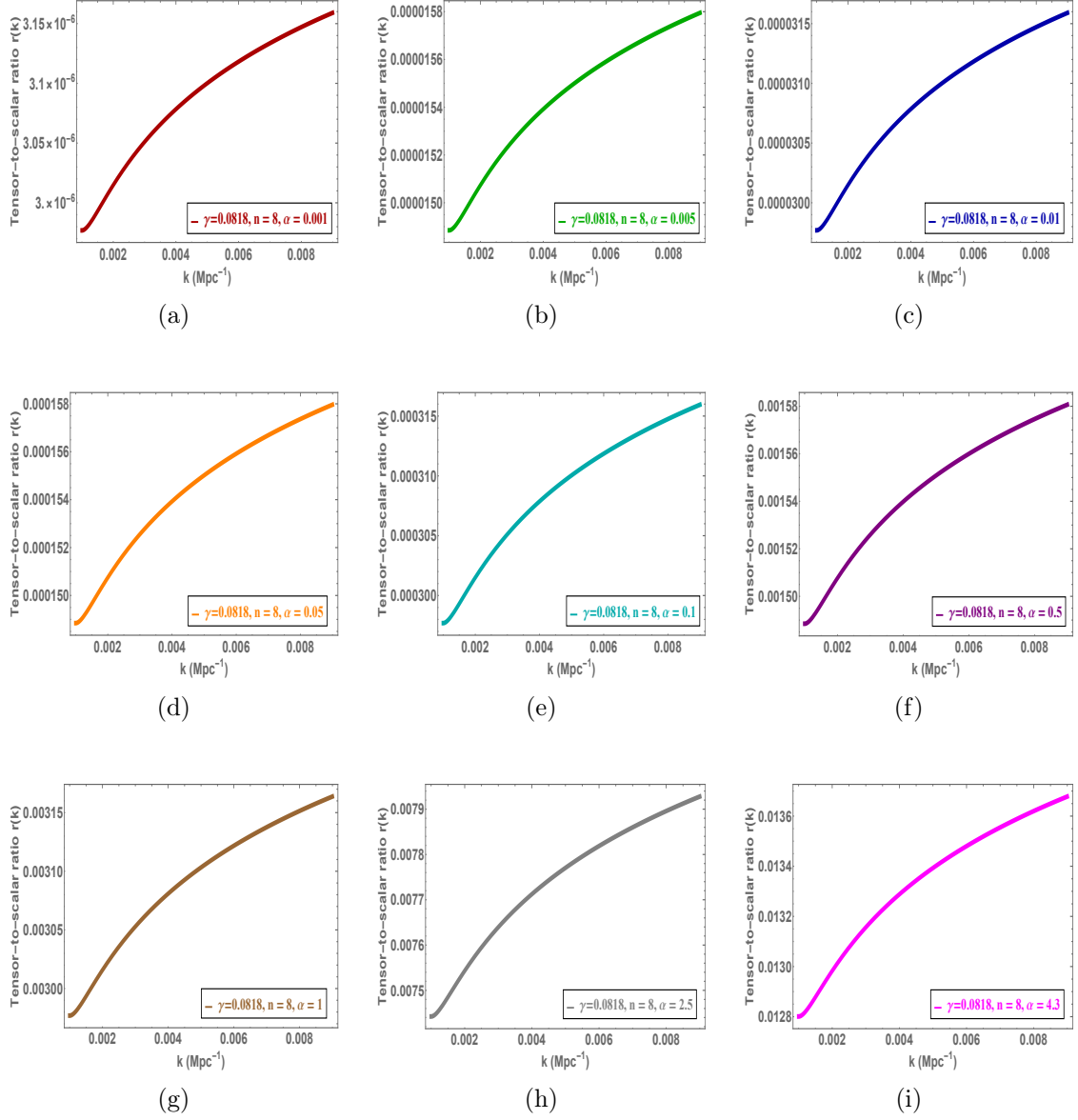


Figure 17. Tensor-to-scalar ratios for nine values of α for $\gamma = 0.0818$ and $n = 8$. The values of $r(k)$ tend to increase with the increase in α at a particular k value.

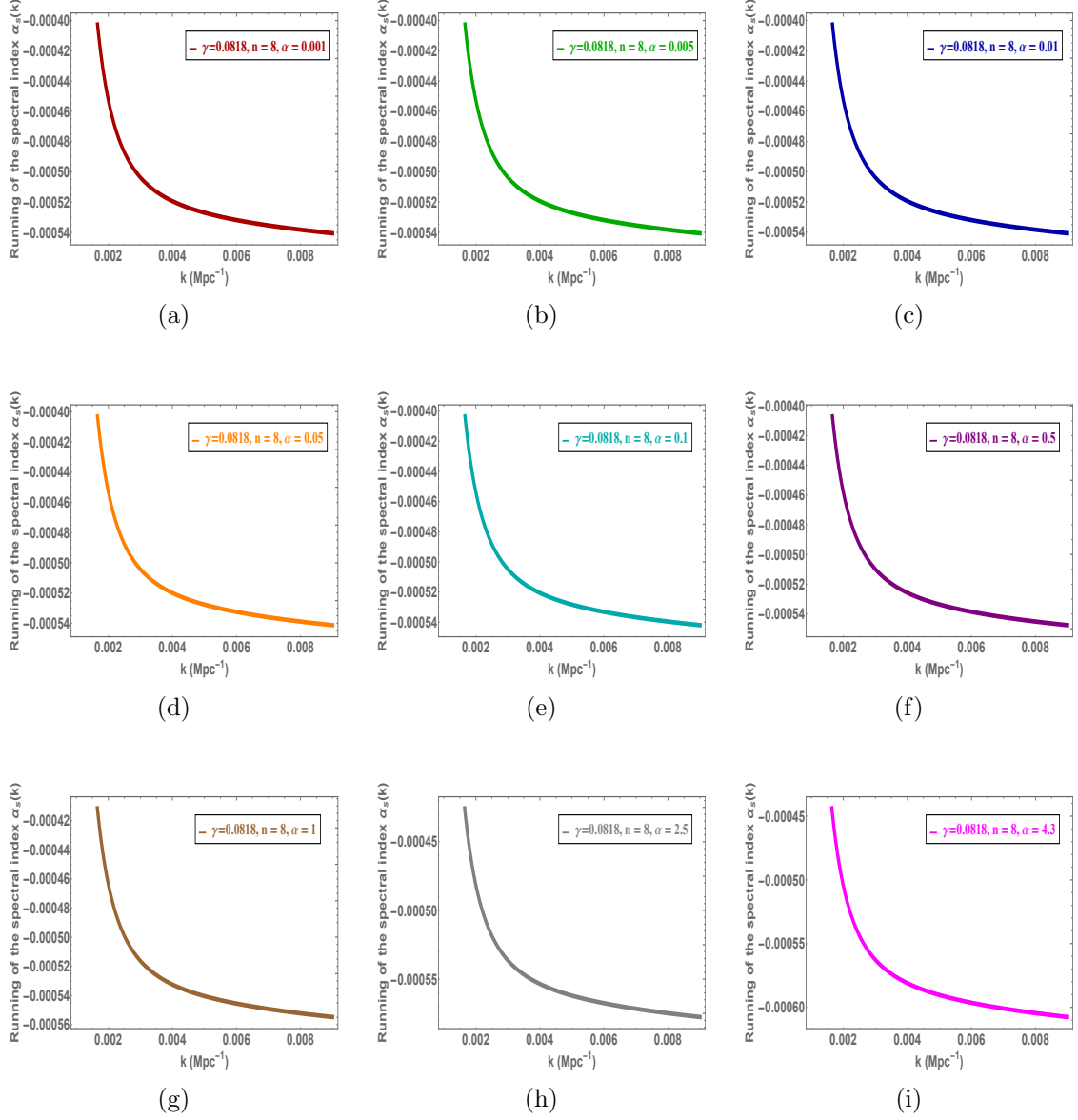


Figure 18. Running of spectral index for nine values of α for $\gamma = 0.0818$ and $n = 8$. The values of $\alpha_s(k)$ do not vary significantly with the increase in α at a particular k value.

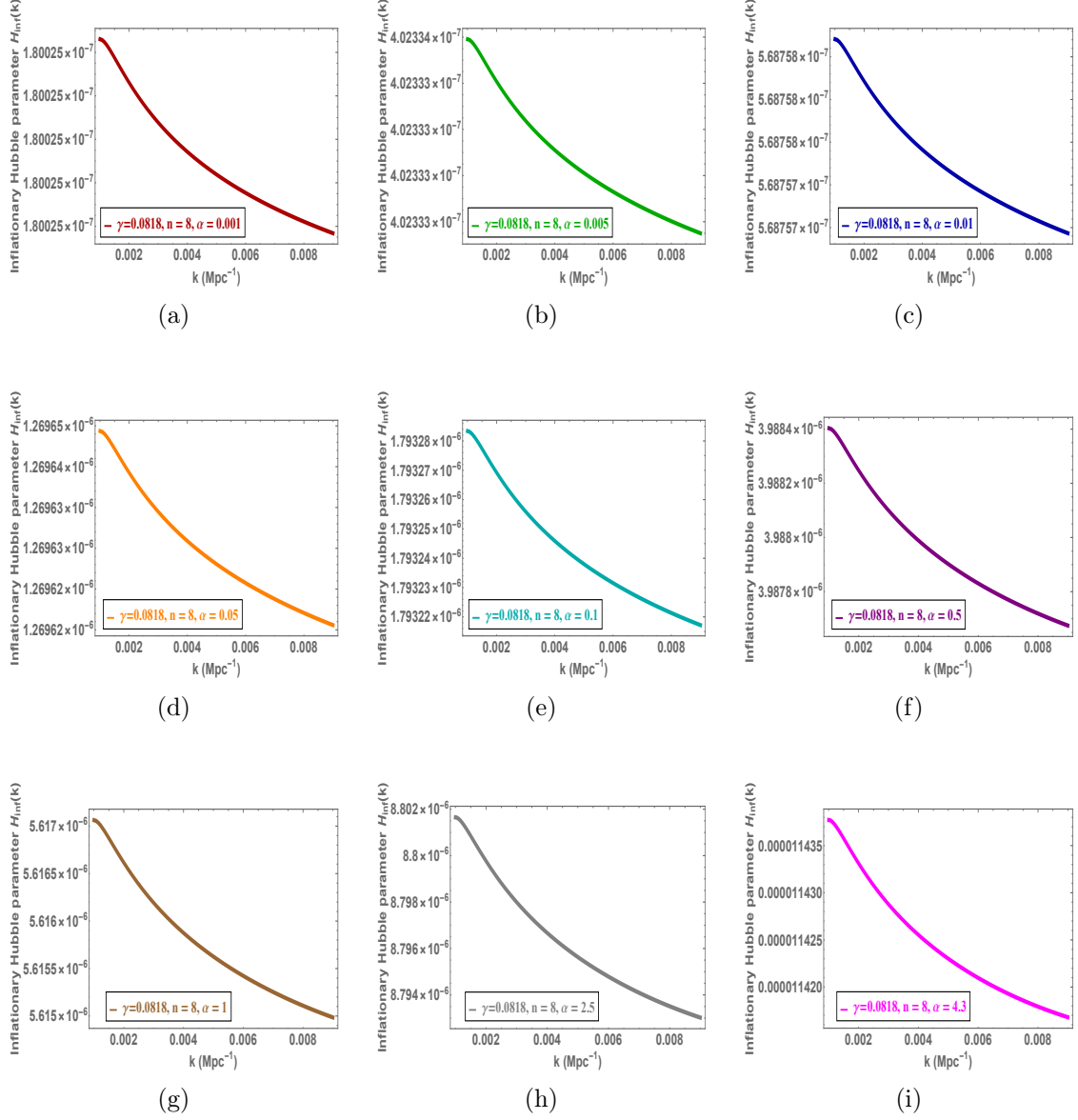


Figure 19. Inflationary Hubble parameters for nine values of α for $\gamma = 0.0818$ and $n = 8$. The values of $H(k)$ tend to increase with the increase in α at a particular k -value.

4.4 Role of ESP in constraining the parameter α

Now, we decode the unusual behaviour of $\xi^{(0)}(k)$ with k within $0.05 \leq \alpha \leq 4.3$. Let us begin with the expressions of number of remaining e-folds of Eqs. (3.6) and (3.7). It is enough to satisfy the inflationary data of Planck around 60-e-folds and it is sufficient to consider a single field slow-roll inflation.

Here we denote ξ for $N = 63.49$ at $k = 0.001 \text{ Mpc}^{-1}$ as ξ_* , which depends on three model parameters *viz.*, n , γ and α . For particular values of n and γ , ξ_* is a complicated function of α ,

$$\xi_*(\alpha) = \sqrt{\frac{3\alpha}{2}} \ln \left(\frac{4n\gamma N e^{-n}}{3\alpha} \right). \quad (4.7)$$

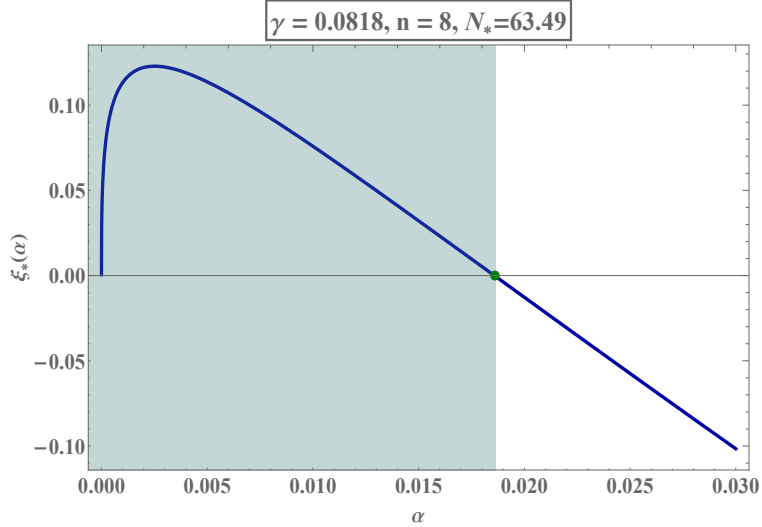


Figure 20. Variation of ξ_* with α for a fixed set of model parameters. The shaded region describes the allowed range of α for which $\xi_* > 0$.

In figure 20, $\xi_*(\alpha)$ is plotted against α for the chosen model parameters, $\gamma = 0.0818$ and $n = 8$. As α increases, ξ_* increases, reaches a maximum value and then monotonically decreases. After a certain value of α (denoted by a red dot) *viz.*, $\alpha = 0.0186$, it becomes negative and does not return to positive value. Such kind of behaviour we have noticed in figures 8a - 8i. Now, as discussed in Section 2, the inflation takes place for $\xi > 0$ region above the Enhanced Symmetry Point (ESP) at $\xi = 0$ (see figure 1). The inflaton field stops rolling after hitting the ESP, remains frozen there for a while behaving like EDE and then freely falls rapidly through the steepest portion of the potential during kination until it reaches the throat of the potential tail to become DE in the present universe. Therefore, $\xi > 0$ is an indispensable criterion for quintessential inflation. So, from figure 20 and Eq. (4.7) we can infer that the ESP at $\xi = 0$ sets an upper cut-off of α ,

$$\alpha_{\max} = \frac{4n\gamma N e^{-n}}{3} \quad (4.8)$$

beyond which $\xi_* < 0$. In our case, $\alpha_{\max} = 0.0186$. That is why, we obtain negative values of ξ_* from $\alpha = 0.05$ onward in figure 8. Therefore the presence of ESP *vis-à-vis* the EDE restricts α as $\alpha < \alpha_{\max}$. In non-EDE version of quintessential inflation [168], ξ_* is always positive, no matter what value of α is chosen. But in the EDE-version the presence of the factor γe^{-n} bears the signature of EDE, which confines α below α_{\max} . Evidently, this upper limit of α depends on n and γ , which are again constrained by the present-day vacuum density as shown in Eq. (4.5). Thus, apart from setting the correct energy scale for quintessence, the EDE plays a crucial role (albeit, secondary¹⁸) in providing a consistent inflaton potential by constraining the parameter α .

¹⁸Its primary role is to resolve the Hubble tension, staying at the post inflationary regime.

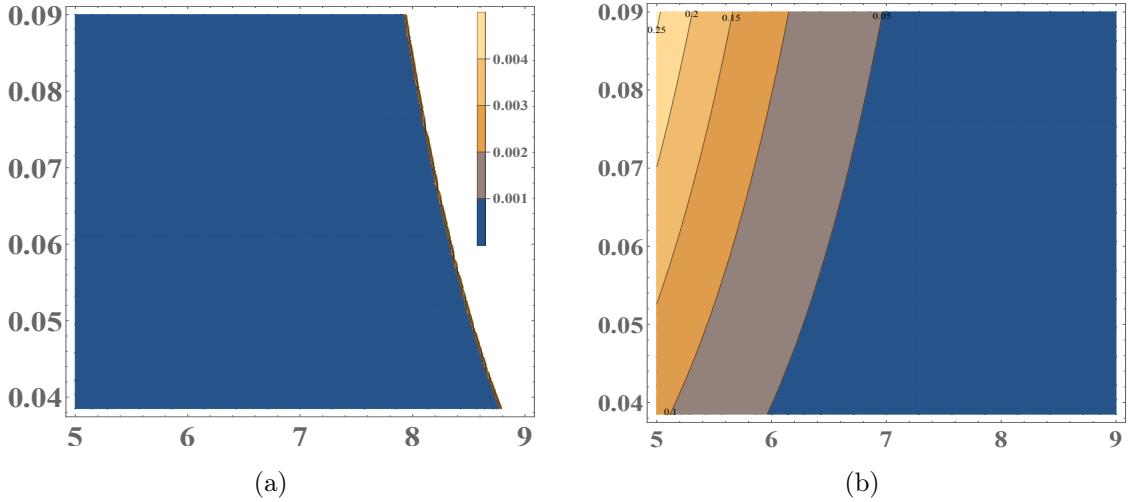


Figure 21. Contour plots of γ vs. n with respect to M (left) according to Eq. (4.5) and α_{\max} (right) according to Eq. (4.8) around the chosen values of n and γ . The vertical bar in figure 21a shows the scale for the obtained values of M (see table 1). In this figure the $\gamma - n$ boundary signifies that the favourable values lie within a region restricted by $n \in [8, 9)$ and $\gamma \in [0.035, 0.09]$ and below these ranges γ and n are independent of each other. The coloured regions in figure 21b represent the corresponding values of α_{\max} , indicated at the end of the respective boundaries.

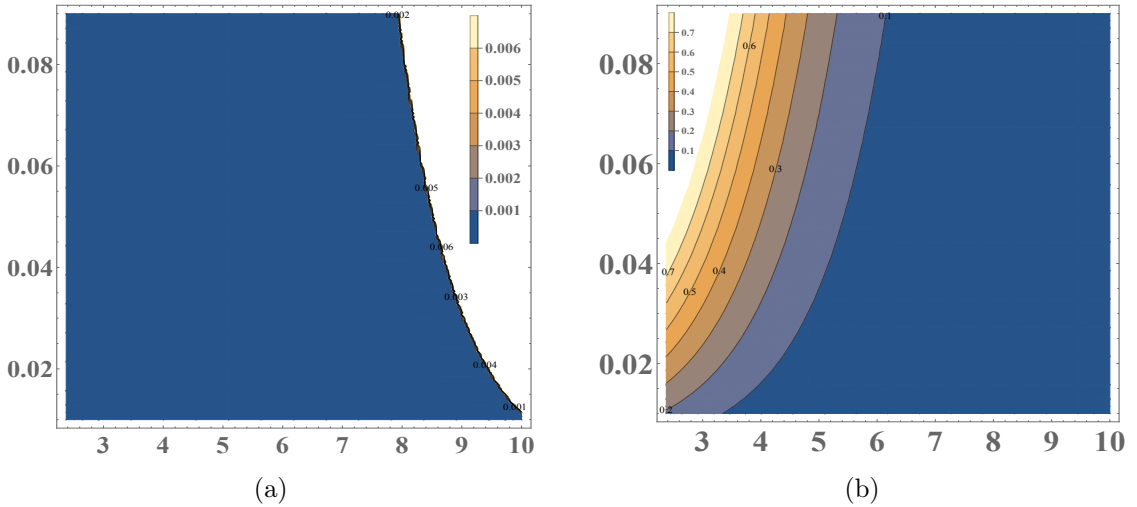


Figure 22. Contour plots of γ vs. n with respect to M (left) according to Eq. (4.5) and α_{\max} (right) according to Eq. (4.8) about broad ranges of values of n and γ . The vertical bar in figure 22a shows the scale for the Planck-supported values of M (see table 1). In this figure the $\gamma - n$ boundary signifies that the favourable values lie within a region restricted by $n \in [8, 10]$ and $\gamma \in [0.01, 0.09]$ and below these ranges γ and n are independent of each other. The coloured regions in figure 22b represent the corresponding values of α_{\max} , indicated at the end of the respective boundaries.

In figures 21 and 22 we show the $\gamma - n$ contour plots with respect to the obtained and Planck-allowed values of M following Eq. (4.5); and with respect to α_{\max} following Eq. (4.8). It is clear from these plots that $2.4 \leq n \leq 10$ and $0.01 \leq \gamma \leq 0.09$ can be considered as legitimate ranges for n and γ , respectively, in order to support the Planck data. For all

cases the maximum allowed value of α_{\max} is $\sim 10^{-1}$. Figures 21a and 22a show that most of the M -values lie on the $n - \gamma$ boundaries characterised by $n \in [8, 10]$, $\gamma \in [0.01, 0.09]$ and the associated upper limit of α_{\max} is constrained by $\alpha_{\max} < 0.1$. So, we can consider that $8 \leq n \leq 10$, $0.01 \leq \gamma \leq 0.09$ and $\alpha_{\max} < 0.1$ (exact value can be estimated for a specific choices of γ and n from Eq. (4.8)) are the final ranges of the model parameters for the EDE-motivated quintessential α -attractor potential.

So far as the lower limit of α is concerned, it depends on the power of convergence into self-consistent solutions of the mode equations for the assigned value of α as boundary condition. In our case, we find that below $\alpha = 0.001$ no solution is obtained for all possible boundary conditions. Therefore we set the lower limit of α as $\alpha_{\min} = 0.001$. However, it may be different for different quintessential α -attractor models. In Ref. [113] it is found that $\alpha \sim 10^{-3}$ which is the same as the lower limit in our case. So, we can say that $0.001 \leq \alpha < 0.1$ is the final range of α for $8 \leq n \leq 10$ and $0.01 \leq \gamma \leq 0.09$. For the values of n and γ used for mode analysis (see figures 8 - 19) *viz.*, $n = 8$ and $\gamma = 0.0818$, α lies within the range $0.001 \leq \alpha \leq 0.0186$.

Thus, we have constrained the parameter α by two different ways. The lower limit is determined by the consistency checking of the first order perturbative mode equations of the inflaton field and the upper limit is fixed by the ESP in the EDE-motivated quintessential α -attractor model. Within this range of α , cosmological parameters do not get affected appreciably *vis-à-vis* the Planck data. This is one kind of verification of the EDE characteristics [113] by k -space analysis.

4.5 Obtained results in light of PLANCK-2018

We explicitly compare our results for the newly obtained range of α with Planck-2018 data. We take help of the joint marginalised contour plots of n_s versus r generated from the simulation data available in Planck Legacy Archive (<https://pla.esac.esa.int/>) by running in GetDist (<https://getdist.readthedocs.io/en/latest/>) plotting utility and Python Jupyter notebook environment (<https://jupyter.org/>). All these data include the effects of CMB E mode polarisation, lensing and BAO. The estimated values of n_s and r described in subsection 4.3 are used to compare with the Planck data.

Figure 23 shows the results of the comparison between the parameters calculated from the dynamical mode analysis and that of Planck data for three values of α *viz.*, $\alpha = 0.001, 0.005, 0.01$ in the k -modes ranging from $0.001 - 0.009 \text{ Mpc}^{-1}$. Axes of the graphs are reasonably extended to fit the data of r in the y direction. The cumulative mode responses of n_s and r are demonstrated by the yellow lines with two identical dots at the ends. These dots signify that the outputs are derived from a single value of number of remaining e-folds *i.e.* $N = 63.49$ as initial condition in the entire k -space. Blue and red areas in the graphs indicate the 68% and 95% CL zones respectively. All the yellow lines lie within 68% CL for the given values of α and no results are found to exist beyond that. As α increases from 0.001 up to 0.01, the line segments are lifted towards higher and higher values of r which is a direct verification of the double pole behaviour of the concerned model.

In Ref. [169] we found that, in ordinary α -attractor E and T models α is restricted between $\alpha = 1$ and $\alpha = 15$ in discrete manner. $\alpha \leq 10$ and $\alpha = 15$ results lie within 68% and 95% CL zones respectively. This range of α becomes more stringent on coupling the quintessence in the inflationary framework in order to explain both the early and late-time expansions of the universe. In Ref. [168] we found that the upper and lower bounds of α are confined between $\alpha = 4.3$ and 0.1 in continuous fashion. It may be noted that the fractional

values of α are important requirements for the α -attractor formulation in minimal $\mathcal{N} = 1$ [174] and maximal $\mathcal{N} = 8$ [196] supergravity theories.

The present work shows that, α is restricted in the closed interval [0.001, 0.0186]. The lower bound of α , which was set to $\alpha = 0.1$ in earlier case, now becomes $\alpha = 0.001$. Therefore around hundred order of magnitude is dropped by the attachment of EDE with quintessence. Such a tiny values of α are currently reported in [113] to resolve the Hubble tension. Also, these extremely low limits of α are the new B -mode targets of ongoing and upcoming LSS surveys [221–240].

In the last figure 24 we merge all the plots of figure 23. Each coloured line represents the results for a particular value of α . The spectral tilts of all the lines are described by the negative and positive mode variations of n_s and r , respectively. The tilts are such that the results always lie within the regime of 68% CL. This reveals that the potential considered in this paper is a single field concave type having a long slow-roll plateau. The increasing behaviour of the parametric lines stops within the blue zone signifying the fact that the model is always a slow-roll one *i.e.* Planck supported for all values of the model parameters.

On the whole, we believe that the model, considered here, has the efficacy to explain inflation, quintessence and the EDE in unified way.

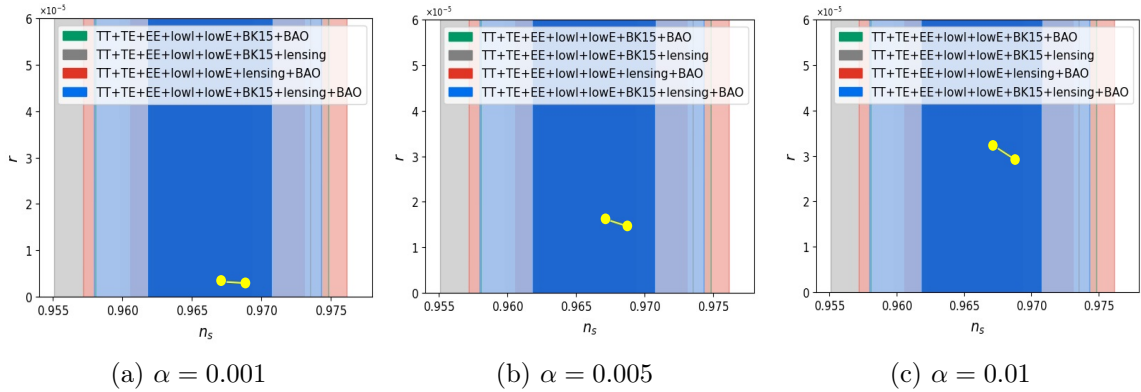


Figure 23. Comparisons of all the calculated values of n_s and r with the Planck constraints for first three values of α . As α increases the parametric line is shifted upwards but does not cross the boundary of 68% CL. The yellow bubbles at the ends represent that all the values in the graphs are computed from the number of remaining e-folds $N = 63.49$.

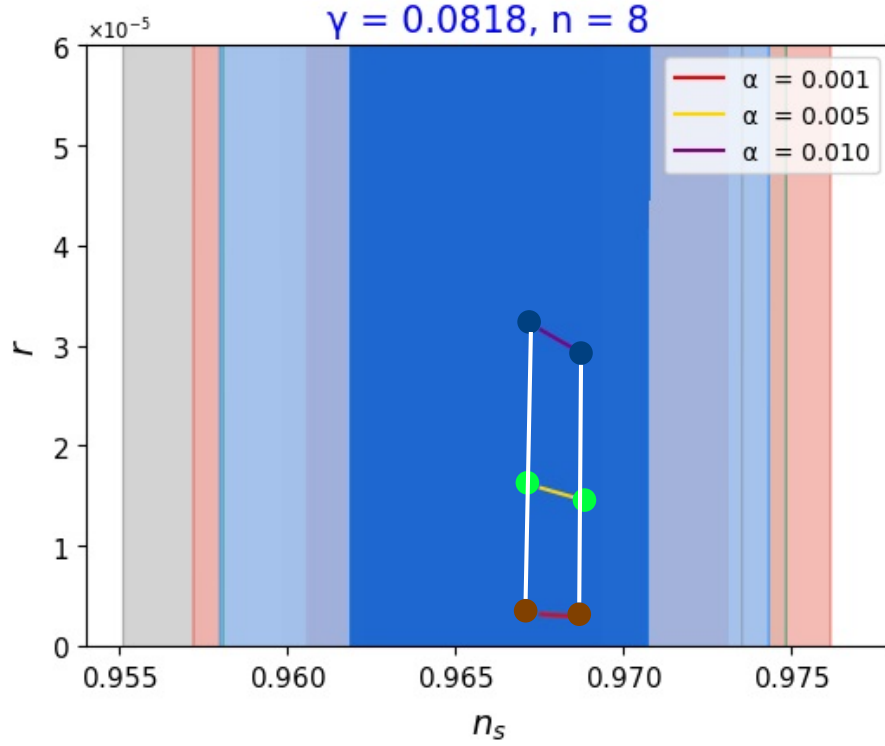


Figure 24. Combined results of figure 23 for all three values of α . White line signifies that all possible values of α are permitted between two extreme limits. The slopes of the lines indicate that the potential is always concave in nature.

4.6 A remark on the resolution of the Hubble tension

In the present paper, we do not intend to solve the Hubble tension, rather our aim is to constrain the model parameters (n, γ, α) , specifically α , from the aspects of ESP *vis-à-vis* the EDE in the inflationary dynamics in the light of Planck+BICEP2/Keck results. However, we can get a very rough idea about the estimations of the model parameters, which can be helpful in the resolution of the Hubble tension.

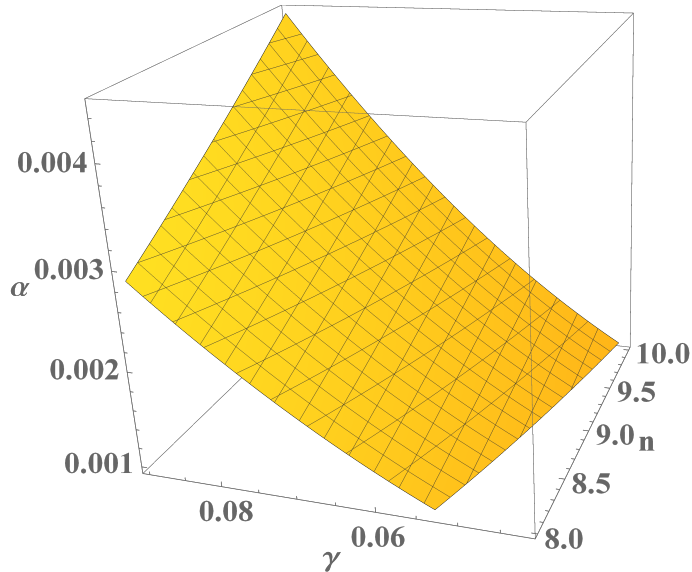


Figure 25. Three dimensional contour plot of n , γ and α for Eq. (4.9). The plot shows the necessary ranges of the model parameters for having the required value of $\Omega_{\text{equal}} (\approx 0.1)$ for the resolution of H_0 tension.

As discussed in Section 2, the ξ -field behaves as the EDE as long as it is trapped at the ESP during a time, which includes starting of formation of radiation and matter and then matter-radiation equality, before CMB decoupling. Once the density parameter reaches its maximum value Ω_{equal} , the field unfreezes and undergoes a free-fall in kination period to appear at the quintessential runaway to become (late) dark energy at present time. Now, as indicated in Refs. [113, 114, 140], in order to resolve the Hubble tension we should have $\Omega_{\text{equal}} = 0.10 \pm 0.02 \simeq 0.1$ *i.e.* $\rho_{\xi}(0)$ should be about 10% of the total density of the universe during equality at redshift 4070_{-840}^{+400} [114]. Following this idea we can further constrain the model parameters using Eq. (2.14) as follows. The three dimensional contour plot of the equation

$$\Omega_{\text{equal}} = \frac{18\alpha}{(n\gamma)^2} = 0.1 \quad (4.9)$$

in figure 25 shows that, in order to have the required value of density parameter at equality, the model parameters should be within the following range: $8 \leq n \leq 10$, $0.04 \leq \gamma \leq 0.09$ and $0.001 \leq \alpha \leq 0.0045$. Therefore, for the EDE motivated quintessential α -attractor inflaton potential considered here, the ranges of γ and α are further tightened over the ranges found by the mode analysis and the α -cut-off, described in previous subsection, to solve the H_0 tension. However, a full simulation, based on statistical analysis (like MCMC), is required for actual results using post inflationary attributes. See [113] as an example. It is at least clear, here, that the parameter α should be $\sim 10^{-3}$ for building up a successful model for the EDE-motivated quintessential α -attractor inflation in conjunction with the resolution of the Hubble tension.

5 Conclusions

In conclusion, we have,

1. constructed a new version of quintessential α -attractor potential with EDE of non-oscillating type. The potential comprises two asymptotic poles corresponding to the inflationary slow-roll plateau and the quintessential tail, a steep slope for kinetically driven free fall and an ESP at the origin,
2. studied in details the scalar field dynamics of inflation near pole boundaries and the geometric structure of the inflaton potential, featuring the aspects of EDE,
3. extracted two regimes of operation by successive approximations in field space corresponding to inflation and quintessence,
4. performed a first-order quantum mode analysis of the inflaton perturbation by DHE method in a perturbed metric background,
5. examined the mode responses of the cosmological parameters for $k = 0.001 - 0.009 \text{ Mpc}^{-1}$ for $\gamma = 0.0818$, $n = 8$ and nine values of α within $\alpha = 0.001 - 4.3$. The estimated values of the parameters satisfy Planck-2018+BICEP2/Keck-2015 data at 68% CL,
6. employed the variations of n_s and r in k -space in order to probe their cumulative mode behaviour in $n_s - r$ parametric space of Planck. The resulting line segments mimic the double-pole feature of the model and the associated spectral tilts show that the obtained results lie always within 68% CL zone for all values of the model parameters,
7. verified that from observational viewpoint, EDE has no effect on the cosmological parameters, which is one of the rudimentary property of EDE. But its presence in the model manifests in two ways. One is in the improved values of some parameters compared to the earlier ones [168, 169], specifically the energy scales of inflation M and the EDE-modified present day vacuum density V_Λ^{exact} . Their improved values are found to be $M = 5.58 \times 10^{-4} - 4.57 \times 10^{-3} M_P$ and $V_\Lambda^{\text{exact}} = 1.042 \times 10^{-119} - 4.688 \times 10^{-116} M_P^4$. These values satisfy the required COBE/Planck normalization and the experimental value of vacuum density $V_\Lambda^{\text{Planck}} \sim 10^{-120} M_P^4$. The second one is in the presence of ESP at the origin in the potential and thereby making the inflaton field positive ($\xi > 0$), and
8. finally, constrained the crucial parameter α by two different methods. The upper limit is fixed by a new probe *viz.*, the ESP of the potential and the lower limit is determined by the consistent initial conditions of first order perturbative mode equations of the inflaton field. We find that α should be within $0.001 \leq \alpha < 0.1$ continuously for γ and n lying within $0.01 \leq \gamma \leq 0.09$ and $8 \leq n \leq 10$ respectively. For the chosen values of the model parameters *i.e.* $\gamma = 0.0818$ and $n = 8$, the range of α is obtained as $0.001 \leq \alpha \leq 0.0186$. The lower and upper limits are substantially diminished from 0.1 to 0.001 and 4.3 to 0.0186, respectively, in comparison to the earlier model in Ref. [168], by the incorporation of the EDE in quintessential inflaton field. We have also found by an approximate calculations that, in order to resolve the Hubble tension the ranges of γ and α are further restricted to $0.04 \leq \gamma \leq 0.09$ and $0.001 \leq \alpha \leq 0.0045$. Therefore, lower end of α is capable of resolving the H_0 discrepancy, as also described in Ref. [113]. However, the entire space of α is essential for studying the early and late-time signatures of spacetime expansion of the universe.

Acknowledgments

The authors acknowledge the University Grants Commission, The Government of India for the CAS-II program in the Department of Physics, The University of Burdwan. AS acknowledges The Government of West Bengal for granting him the Swami Vivekananda fellowship.

References

- [1] **WMAP** Collaboration, G. Hinshaw *et al.*, “Nine-Year Wilkinson Microwave Anisotropy Probe (WMAP) Observations: Cosmological Parameter Results,” *Astrophys. J. Suppl.* **208** (2013) 19, [arXiv:1212.5226 \[astro-ph.CO\]](#).
- [2] D. Huterer and M. S. Turner, “Prospects for probing the dark energy via supernova distance measurements,” *Phys. Rev. D* **60** (1999) 081301, [arXiv:astro-ph/9808133](#).
- [3] **Supernova Search Team** Collaboration, A. G. Riess *et al.*, “Observational evidence from supernovae for an accelerating universe and a cosmological constant,” *Astron. J.* **116** (1998) 1009–1038, [arXiv:astro-ph/9805201](#).
- [4] **Supernova Cosmology Project** Collaboration, S. Perlmutter *et al.*, “Measurements of Ω and Λ from 42 high redshift supernovae,” *Astrophys. J.* **517** (1999) 565–586, [arXiv:astro-ph/9812133](#).
- [5] **Planck** Collaboration, P. A. R. Ade *et al.*, “Planck 2015 results. XIII. Cosmological parameters,” *Astron. Astrophys.* **594** (2016) A13, [arXiv:1502.01589 \[astro-ph.CO\]](#).
- [6] **Planck** Collaboration, P. A. R. Ade *et al.*, “Planck 2015 results. XX. Constraints on inflation,” *Astron. Astrophys.* **594** (2016) A20, [arXiv:1502.02114 \[astro-ph.CO\]](#).
- [7] **Planck** Collaboration, N. Aghanim *et al.*, “Planck 2018 results. VI. Cosmological parameters,” *Astron. Astrophys.* **641** (2020) A6, [arXiv:1807.06209 \[astro-ph.CO\]](#). [Erratum: *Astron. Astrophys.* 652, C4 (2021)].
- [8] **Planck** Collaboration, Y. Akrami *et al.*, “Planck 2018 results. X. Constraints on inflation,” *Astron. Astrophys.* **641** (2020) A10, [arXiv:1807.06211 \[astro-ph.CO\]](#).
- [9] **KiDS** Collaboration, M. Asgari *et al.*, “KiDS-1000 Cosmology: Cosmic shear constraints and comparison between two point statistics,” *Astron. Astrophys.* **645** (2021) A104, [arXiv:2007.15633 \[astro-ph.CO\]](#).
- [10] **DES** Collaboration, T. M. C. Abbott *et al.*, “Dark Energy Survey Year 3 results: Cosmological constraints from galaxy clustering and weak lensing,” *Phys. Rev. D* **105** no. 2, (2022) 023520, [arXiv:2105.13549 \[astro-ph.CO\]](#).
- [11] R. R. Caldwell, R. Dave, and P. J. Steinhardt, “Cosmological imprint of an energy component with general equation of state,” *Phys. Rev. Lett.* **80** (1998) 1582–1585, [arXiv:astro-ph/9708069](#).
- [12] P. J. E. Peebles and B. Ratra, “The Cosmological Constant and Dark Energy,” *Rev. Mod. Phys.* **75** (2003) 559–606, [arXiv:astro-ph/0207347](#).
- [13] B. Ratra and P. J. E. Peebles, “Cosmological Consequences of a Rolling Homogeneous Scalar Field,” *Phys. Rev. D* **37** (1988) 3406.
- [14] E. J. Copeland, M. Sami, and S. Tsujikawa, “Dynamics of dark energy,” *Int. J. Mod. Phys. D* **15** (2006) 1753–1936, [arXiv:hep-th/0603057](#).
- [15] S. Weinberg, “The Cosmological Constant Problem,” *Rev. Mod. Phys.* **61** (1989) 1–23.
- [16] K. Dimopoulos, *Introduction to Cosmic Inflation and Dark Energy*. CRC Press, 5, 2022.

- [17] S. del Campo, R. Herrera, and D. Pavon, “Interacting models may be key to solve the cosmic coincidence problem,” *JCAP* **01** (2009) 020, [arXiv:0812.2210 \[gr-qc\]](#).
- [18] G. Huey and B. D. Wandelt, “Interacting quintessence. The Coincidence problem and cosmic acceleration,” *Phys. Rev. D* **74** (2006) 023519, [arXiv:astro-ph/0407196](#).
- [19] H. E. S. Velten, R. F. vom Marttens, and W. Zimdahl, “Aspects of the cosmological ‘coincidence problem’,” *Eur. Phys. J. C* **74** no. 11, (2014) 3160, [arXiv:1410.2509 \[astro-ph.CO\]](#).
- [20] B. Wang, E. Abdalla, F. Atrio-Barandela, and D. Pavon, “Dark Matter and Dark Energy Interactions: Theoretical Challenges, Cosmological Implications and Observational Signatures,” *Rept. Prog. Phys.* **79** no. 9, (2016) 096901, [arXiv:1603.08299 \[astro-ph.CO\]](#).
- [21] Y. L. Bolotin, A. Kostenko, O. A. Lemets, and D. A. Yerokhin, “Cosmological Evolution With Interaction Between Dark Energy And Dark Matter,” *Int. J. Mod. Phys. D* **24** no. 03, (2014) 1530007, [arXiv:1310.0085 \[astro-ph.CO\]](#).
- [22] I. Zlatev, L.-M. Wang, and P. J. Steinhardt, “Quintessence, cosmic coincidence, and the cosmological constant,” *Phys. Rev. Lett.* **82** (1999) 896–899, [arXiv:astro-ph/9807002](#).
- [23] B. Spokoiny, “Deflationary universe scenario,” *Phys. Lett. B* **315** (1993) 40–45, [arXiv:gr-qc/9306008](#).
- [24] C. Pallis, “Quintessential kination and cold dark matter abundance,” *JCAP* **10** (2005) 015, [arXiv:hep-ph/0503080](#).
- [25] C. Pallis, “Kination-dominated reheating and cold dark matter abundance,” *Nucl. Phys. B* **751** (2006) 129–159, [arXiv:hep-ph/0510234](#).
- [26] M. E. Gomez, S. Lola, C. Pallis, and J. Rodriguez-Quintero, “Quintessential Kination and Thermal Production of Gravitinos and Axinos,” *JCAP* **01** (2009) 027, [arXiv:0809.1859 \[hep-ph\]](#).
- [27] P. J. E. Peebles and A. Vilenkin, “Quintessential inflation,” *Phys. Rev. D* **59** (1999) 063505, [arXiv:astro-ph/9810509](#).
- [28] M. Peloso and F. Rosati, “On the construction of quintessential inflation models,” *JHEP* **12** (1999) 026, [arXiv:hep-ph/9908271](#).
- [29] A. A. Sen, I. Chakrabarty, and T. R. Seshadri, “Quintessential inflation with dissipative fluid,” *Gen. Rel. Grav.* **34** (2002) 477–490, [arXiv:gr-qc/0005104](#).
- [30] A. B. Kaganovich, “Field theory model giving rise to ‘quintessential inflation’ without the cosmological constant and other fine tuning problems,” *Phys. Rev. D* **63** (2001) 025022, [arXiv:hep-th/0007144](#).
- [31] M. Yahiro, G. J. Mathews, K. Ichiki, T. Kajino, and M. Orito, “Constraints on cosmic quintessence and quintessential inflation,” *Phys. Rev. D* **65** (2002) 063502, [arXiv:astro-ph/0106349](#).
- [32] J. Martin and M. A. Musso, “Stochastic quintessence,” *Phys. Rev. D* **71** (2005) 063514, [arXiv:astro-ph/0410190](#).
- [33] G. Barenboim and J. D. Lykken, “Slinky Inflation,” *Phys. Lett. B* **633** (2006) 453–457, [arXiv:astro-ph/0504090](#).
- [34] R. Rosenfeld and J. A. Frieman, “A Simple model for quintessential inflation,” *JCAP* **09** (2005) 003, [arXiv:astro-ph/0504191](#).
- [35] V. H. Cardenas, “Tachyonic quintessential inflation,” *Phys. Rev. D* **73** (2006) 103512, [arXiv:gr-qc/0603013](#).
- [36] J. C. Bueno Sanchez and K. Dimopoulos, “Trapped Quintessential Inflation,” *Phys. Lett. B* **642** (2006) 294–301, [arXiv:hep-th/0605258](#). [Erratum: *Phys.Lett.B* 647, 526 (2007)].

- [37] A. Membrilla and M. Bellini, “Quintessential inflation from a variable cosmological constant in a 5D vacuum,” *Phys. Lett. B* **641** (2006) 125–129, [arXiv:gr-qc/0606119](#).
- [38] R. Rosenfeld and J. A. Frieman, “Cosmic microwave background and large-scale structure constraints on a simple quintessential inflation model,” *Phys. Rev. D* **75** (2007) 043513, [arXiv:astro-ph/0611241](#).
- [39] I. P. Neupane, “Reconstructing a model of quintessential inflation,” *Class. Quant. Grav.* **25** (2008) 125013, [arXiv:0706.2654 \[hep-th\]](#).
- [40] M. Bastero-Gil, A. Berera, B. M. Jackson, and A. Taylor, “Hybrid Quintessential Inflation,” *Phys. Lett. B* **678** (2009) 157–163, [arXiv:0905.2937 \[hep-ph\]](#).
- [41] E. Piedipalumbo, P. Scudellaro, G. Esposito, and C. Rubano, “On quintessential cosmological models and exponential potentials,” *Gen. Rel. Grav.* **44** (2012) 2611–2643, [arXiv:1112.0502 \[astro-ph.CO\]](#).
- [42] C. Wetterich, “Inflation, quintessence, and the origin of mass,” *Nucl. Phys. B* **897** (2015) 111–178, [arXiv:1408.0156 \[hep-th\]](#).
- [43] M. W. Hossain, R. Myrzakulov, M. Sami, and E. N. Saridakis, “Variable gravity: A suitable framework for quintessential inflation,” *Phys. Rev. D* **90** no. 2, (2014) 023512, [arXiv:1402.6661 \[gr-qc\]](#).
- [44] M. W. Hossain, R. Myrzakulov, M. Sami, and E. N. Saridakis, “Class of quintessential inflation models with parameter space consistent with BICEP2,” *Phys. Rev. D* **89** no. 12, (2014) 123513, [arXiv:1404.1445 \[gr-qc\]](#).
- [45] M. W. Hossain, R. Myrzakulov, M. Sami, and E. N. Saridakis, “Evading Lyth bound in models of quintessential inflation,” *Phys. Lett. B* **737** (2014) 191–195, [arXiv:1405.7491 \[gr-qc\]](#).
- [46] C.-Q. Geng, M. W. Hossain, R. Myrzakulov, M. Sami, and E. N. Saridakis, “Quintessential inflation with canonical and noncanonical scalar fields and Planck 2015 results,” *Phys. Rev. D* **92** no. 2, (2015) 023522, [arXiv:1502.03597 \[gr-qc\]](#).
- [47] M. Wali Hossain, R. Myrzakulov, M. Sami, and E. N. Saridakis, “Unification of inflation and dark energy à la quintessential inflation,” *Int. J. Mod. Phys. D* **24** no. 05, (2015) 1530014, [arXiv:1410.6100 \[gr-qc\]](#).
- [48] J. Haro and S. Pan, “Bulk viscous quintessential inflation,” *Int. J. Mod. Phys. D* **27** no. 05, (2018) 1850052, [arXiv:1512.03033 \[gr-qc\]](#).
- [49] J. de Haro, “On the viability of quintessential inflation models from observational data,” *Gen. Rel. Grav.* **49** no. 1, (2017) 6, [arXiv:1602.07138 \[gr-qc\]](#).
- [50] J. de Haro, J. Amorós, and S. Pan, “Simple inflationary quintessential model II: Power law potentials,” *Phys. Rev. D* **94** no. 6, (2016) 064060, [arXiv:1607.06726 \[gr-qc\]](#).
- [51] E. Guendelman, E. Nissimov, and S. Pacheva, “Quintessential Inflation, Unified Dark Energy and Dark Matter, and Higgs Mechanism,” *Bulg. J. Phys.* **44** no. 1, (2017) 015–030, [arXiv:1609.06915 \[gr-qc\]](#).
- [52] J. Rubio and C. Wetterich, “Emergent scale symmetry: Connecting inflation and dark energy,” *Phys. Rev. D* **96** no. 6, (2017) 063509, [arXiv:1705.00552 \[gr-qc\]](#).
- [53] S. Ahmad, R. Myrzakulov, and M. Sami, “Relic gravitational waves from Quintessential Inflation,” *Phys. Rev. D* **96** no. 6, (2017) 063515, [arXiv:1705.02133 \[gr-qc\]](#).
- [54] J. Haro, W. Yang, and S. Pan, “Reheating in quintessential inflation via gravitational production of heavy massive particles: A detailed analysis,” *JCAP* **01** (2019) 023, [arXiv:1811.07371 \[gr-qc\]](#).
- [55] D. Bettoni, G. Domènech, and J. Rubio, “Gravitational waves from global cosmic strings in quintessential inflation,” *JCAP* **02** (2019) 034, [arXiv:1810.11117 \[astro-ph.CO\]](#).

- [56] J. Selvaganapathy, “Pure natural quintessential inflation and dark energy,” *Int. J. Mod. Phys. A* **35** no. 19, (2020) 2050097, [arXiv:1911.10466 \[hep-ph\]](#).
- [57] G. B. F. Lima and R. O. Ramos, “Unified early and late Universe cosmology through dissipative effects in steep quintessential inflation potential models,” *Phys. Rev. D* **100** no. 12, (2019) 123529, [arXiv:1910.05185 \[astro-ph.CO\]](#).
- [58] K. Kleidis and V. K. Oikonomou, “A Study of an Einstein Gauss-Bonnet Quintessential Inflationary Model,” *Nucl. Phys. B* **948** (2019) 114765, [arXiv:1909.05318 \[gr-qc\]](#).
- [59] J. Haro, J. Amorós, and S. Pan, “Scaling solutions in quintessential inflation,” *Eur. Phys. J. C* **80** no. 5, (2020) 404, [arXiv:1908.01516 \[gr-qc\]](#).
- [60] D. Benisty and E. I. Guendelman, “Lorentzian Quintessential Inflation,” *Int. J. Mod. Phys. D* **29** no. 14, (2020) 2042002, [arXiv:2004.00339 \[astro-ph.CO\]](#).
- [61] D. Benisty, E. I. Guendelman, E. Nissimov, and S. Pacheva, “Quintessential Inflation with Dynamical Higgs Generation as an Affine Gravity,” *Symmetry* **12** (2020) 734, [arXiv:2003.04723 \[gr-qc\]](#).
- [62] J. de Haro and L. A. Saló, “A Review of Quintessential Inflation,” *Galaxies* **9** no. 4, (2021) 73, [arXiv:2108.11144 \[gr-qc\]](#).
- [63] K. Dimopoulos, “Jointly modelling Cosmic Inflation and Dark Energy,” *J. Phys. Conf. Ser.* **2105** no. 1, (2021) 012001, [arXiv:2106.14966 \[gr-qc\]](#).
- [64] S. X. Tian and Z.-H. Zhu, “Cosmological consequences of a scalar field with oscillating equation of state. III. Unifying inflation with dark energy and small tensor-to-scalar ratio,” *Phys. Rev. D* **103** no. 12, (2021) 123545, [arXiv:2106.14002 \[astro-ph.CO\]](#).
- [65] L. Aresté Saló, D. Benisty, E. I. Guendelman, and J. de Haro, “ α -attractors in quintessential inflation motivated by supergravity,” *Phys. Rev. D* **103** no. 12, (2021) 123535, [arXiv:2103.07892 \[astro-ph.CO\]](#).
- [66] Y. Akrami, S. Casas, S. Deng, and V. Vardanyan, “Quintessential α -attractor inflation: forecasts for Stage IV galaxy surveys,” *JCAP* **04** (2021) 006, [arXiv:2010.15822 \[astro-ph.CO\]](#).
- [67] C. García-García, P. Ruíz-Lapuente, D. Alonso, and M. Zumalacárregui, “ α -attractor dark energy in view of next-generation cosmological surveys,” *JCAP* **07** (2019) 025, [arXiv:1905.03753 \[astro-ph.CO\]](#).
- [68] C. García-García, E. V. Linder, P. Ruíz-Lapuente, and M. Zumalacárregui, “Dark energy from α -attractors: phenomenology and observational constraints,” *JCAP* **08** (2018) 022, [arXiv:1803.00661 \[astro-ph.CO\]](#).
- [69] Y. Akrami, R. Kallosh, A. Linde, and V. Vardanyan, “Dark energy, α -attractors, and large-scale structure surveys,” *JCAP* **06** (2018) 041, [arXiv:1712.09693 \[hep-th\]](#).
- [70] Z. Kepluladze and M. Maziashvili, “New take on the inflationary quintessence,” *Phys. Rev. D* **103** no. 6, (2021) 063540, [arXiv:2102.09203 \[astro-ph.CO\]](#).
- [71] K. Dimopoulos and C. Owen, “Quintessential Inflation with α -attractors,” *JCAP* **06** (2017) 027, [arXiv:1703.00305 \[gr-qc\]](#).
- [72] C.-Q. Geng, C.-C. Lee, M. Sami, E. N. Saridakis, and A. A. Starobinsky, “Observational constraints on successful model of quintessential Inflation,” *JCAP* **06** (2017) 011, [arXiv:1705.01329 \[gr-qc\]](#).
- [73] A. Agarwal, R. Myrzakulov, M. Sami, and N. K. Singh, “Quintessential inflation in a thawing realization,” *Phys. Lett. B* **770** (2017) 200–208, [arXiv:1708.00156 \[gr-qc\]](#).
- [74] L. Aresté Saló and J. de Haro, “Quintessential inflation at low reheating temperatures,” *Eur. Phys. J. C* **77** no. 11, (2017) 798, [arXiv:1707.02810 \[gr-qc\]](#).

- [75] J. De Haro and L. Aresté Saló, “Reheating constraints in quintessential inflation,” *Phys. Rev. D* **95** no. 12, (2017) 123501, [arXiv:1702.04212 \[gr-qc\]](#).
- [76] J. Haro, J. Amorós, and S. Pan, “The Peebles - Vilenkin quintessential inflation model revisited,” *Eur. Phys. J. C* **79** no. 6, (2019) 505, [arXiv:1901.00167 \[gr-qc\]](#).
- [77] J. de Haro, S. Pan, and L. Aresté Saló, “Understanding gravitational particle production in quintessential inflation,” *JCAP* **06** (2019) 056, [arXiv:1903.01181 \[gr-qc\]](#).
- [78] D. Benisty and E. I. Guendelman, “Quintessential Inflation from Lorentzian Slow Roll,” *Eur. Phys. J. C* **80** no. 6, (2020) 577, [arXiv:2006.04129 \[astro-ph.CO\]](#).
- [79] M. Shokri, J. Sadeghi, and S. N. Gashti, “Quintessential constant-roll inflation,” *Phys. Dark Univ.* **35** (2022) 100923, [arXiv:2107.04756 \[astro-ph.CO\]](#).
- [80] D. Bettoni and J. Rubio, “Quintessential Inflation: A Tale of Emergent and Broken Symmetries,” *Galaxies* **10** no. 1, (2022) 22, [arXiv:2112.11948 \[astro-ph.CO\]](#).
- [81] N. Jaman and M. Sami, “What Is Needed of a Scalar Field If It Is to Unify Inflation and Late Time Acceleration?,” *Galaxies* **10** no. 2, (2022) 51, [arXiv:2202.06194 \[gr-qc\]](#).
- [82] J. F. Jesus, R. Valentim, A. A. Escobal, S. H. Pereira, and D. Benndorf, “Gaussian processes reconstruction of the dark energy potential,” *JCAP* **11** (2022) 037, [arXiv:2112.09722 \[astro-ph.CO\]](#).
- [83] K. Fujikura, S. Hashiba, and J. Yokoyama, “Generation of neutrino dark matter, baryon asymmetry, and radiation after quintessential inflation,” [arXiv:2210.05214 \[hep-ph\]](#).
- [84] M. Karčiauskas, S. Rusak, and A. Saez, “Quintessential inflation and nonlinear effects of the tachyonic trap mechanism,” *Phys. Rev. D* **105** no. 4, (2022) 043535, [arXiv:2112.11536 \[astro-ph.CO\]](#).
- [85] S. Basak, S. Bhattacharya, M. R. Gangopadhyay, N. Jaman, R. Rangarajan, and M. Sami, “The paradigm of warm quintessential inflation and spontaneous baryogenesis,” *JCAP* **03** no. 03, (2022) 063, [arXiv:2110.00607 \[astro-ph.CO\]](#).
- [86] L. Areste Salo and J. Haro, “Quintessential Inflation for Exponential Type Potentials: Scaling and Tracker Behavior,” *Eur. Phys. J. C* **81** no. 2, (2021) 105, [arXiv:2009.12912 \[gr-qc\]](#).
- [87] P. Q. Hung, “All in the Family: the quintessential kinship between Inflation and Dark Energy,” [arXiv:2306.13703 \[hep-ph\]](#).
- [88] A. Alho and C. Ugla, “Quintessential α -attractor inflation: A dynamical systems analysis,” [arXiv:2306.15326 \[gr-qc\]](#).
- [89] A. G. Riess, S. Casertano, W. Yuan, L. M. Macri, and D. Scolnic, “Large Magellanic Cloud Cepheid Standards Provide a 1% Foundation for the Determination of the Hubble Constant and Stronger Evidence for Physics beyond Λ CDM,” *Astrophys. J.* **876** no. 1, (2019) 85, [arXiv:1903.07603 \[astro-ph.CO\]](#).
- [90] A. G. Riess, S. Casertano, W. Yuan, J. B. Bowers, L. Macri, J. C. Zinn, and D. Scolnic, “Cosmic Distances Calibrated to 1% Precision with Gaia EDR3 Parallaxes and Hubble Space Telescope Photometry of 75 Milky Way Cepheids Confirm Tension with Λ CDM,” *Astrophys. J. Lett.* **908** no. 1, (2021) L6, [arXiv:2012.08534 \[astro-ph.CO\]](#).
- [91] M. G. Dainotti, B. De Simone, T. Schiavone, G. Montani, E. Rinaldi, G. Lambiase, M. Bogdan, and S. Ugale, “On the Evolution of the Hubble Constant with the SNe Ia Pantheon Sample and Baryon Acoustic Oscillations: A Feasibility Study for GRB-Cosmology in 2030,” *Galaxies* **10** no. 1, (2022) 24, [arXiv:2201.09848 \[astro-ph.CO\]](#).
- [92] M. G. Dainotti, B. De Simone, T. Schiavone, G. Montani, E. Rinaldi, and G. Lambiase, “On the Hubble constant tension in the SNe Ia Pantheon sample,” *Astrophys. J.* **912** no. 2, (2021) 150, [arXiv:2103.02117 \[astro-ph.CO\]](#).

- [93] S. Vagnozzi, “New physics in light of the H_0 tension: An alternative view,” *Phys. Rev. D* **102** no. 2, (2020) 023518, [arXiv:1907.07569 \[astro-ph.CO\]](#).
- [94] E. Di Valentino, A. Melchiorri, and O. Mena, “Can interacting dark energy solve the H_0 tension?,” *Phys. Rev. D* **96** no. 4, (2017) 043503, [arXiv:1704.08342 \[astro-ph.CO\]](#).
- [95] E. Di Valentino, A. Melchiorri, O. Mena, and S. Vagnozzi, “Interacting dark energy in the early 2020s: A promising solution to the H_0 and cosmic shear tensions,” *Phys. Dark Univ.* **30** (2020) 100666, [arXiv:1908.04281 \[astro-ph.CO\]](#).
- [96] E. Di Valentino, O. Mena, S. Pan, L. Visinelli, W. Yang, A. Melchiorri, D. F. Mota, A. G. Riess, and J. Silk, “In the realm of the Hubble tension—a review of solutions,” *Class. Quant. Grav.* **38** no. 15, (2021) 153001, [arXiv:2103.01183 \[astro-ph.CO\]](#).
- [97] F.-Y. Cyr-Racine, “Cosmic Expansion: A mini review of the Hubble-Lemaître tension,” in *55th Rencontres de Moriond on Electroweak Interactions and Unified Theories*. 5, 2021. [arXiv:2105.09409 \[astro-ph.CO\]](#).
- [98] R. C. Nunes, S. Vagnozzi, S. Kumar, E. Di Valentino, and O. Mena, “New tests of dark sector interactions from the full-shape galaxy power spectrum,” *Phys. Rev. D* **105** no. 12, (2022) 123506, [arXiv:2203.08093 \[astro-ph.CO\]](#).
- [99] W. Yang, S. Pan, E. Di Valentino, R. C. Nunes, S. Vagnozzi, and D. F. Mota, “Tale of stable interacting dark energy, observational signatures, and the H_0 tension,” *JCAP* **09** (2018) 019, [arXiv:1805.08252 \[astro-ph.CO\]](#).
- [100] L.-F. Wang, J.-H. Zhang, D.-Z. He, J.-F. Zhang, and X. Zhang, “Constraints on interacting dark energy models from time-delay cosmography with seven lensed quasars,” *Mon. Not. Roy. Astron. Soc.* **514** no. 1, (2022) 1433–1440, [arXiv:2102.09331 \[astro-ph.CO\]](#).
- [101] S. Gariazzo, E. Di Valentino, O. Mena, and R. C. Nunes, “Late-time interacting cosmologies and the Hubble constant tension,” *Phys. Rev. D* **106** no. 2, (2022) 023530, [arXiv:2111.03152 \[astro-ph.CO\]](#).
- [102] J.-Q. Jiang, G. Ye, and Y.-S. Piao, “Impact of the Hubble tension on the $r-n_s$ contour,” [arXiv:2303.12345 \[astro-ph.CO\]](#).
- [103] S. A. Adil, O. Akarsu, E. Di Valentino, R. C. Nunes, E. Ozulker, A. A. Sen, and E. Specogna, “Omnipotent dark energy: A phenomenological answer to the Hubble tension,” [arXiv:2306.08046 \[astro-ph.CO\]](#).
- [104] I. Ben-Dayan and U. Kumar, “Theoretical Priors and the Dark Energy Equation of State,” [arXiv:2310.03092 \[astro-ph.CO\]](#).
- [105] S. Pan and W. Yang, “On the interacting dark energy scenarios – the case for Hubble constant tension,” [arXiv:2310.07260 \[astro-ph.CO\]](#).
- [106] M. Lucca, “Dark energy–dark matter interactions as a solution to the S8 tension,” *Phys. Dark Univ.* **34** (2021) 100899, [arXiv:2105.09249 \[astro-ph.CO\]](#).
- [107] R. C. Nunes and S. Vagnozzi, “Arbitrating the S8 discrepancy with growth rate measurements from redshift-space distortions,” *Mon. Not. Roy. Astron. Soc.* **505** no. 4, (2021) 5427–5437, [arXiv:2106.01208 \[astro-ph.CO\]](#).
- [108] E. Di Valentino *et al.*, “Cosmology Intertwined III: $f\sigma_8$ and S_8 ,” *Astropart. Phys.* **131** (2021) 102604, [arXiv:2008.11285 \[astro-ph.CO\]](#).
- [109] I. Ben-Dayan and U. Kumar, “Emergent Unparticles Dark Energy can restore cosmological concordance,” [arXiv:2302.00067 \[astro-ph.CO\]](#).
- [110] M. A. van der Westhuizen and A. Abebe, “Interacting dark energy: clarifying the cosmological implications and viability conditions,” other thesis, 2, 2023.

- [111] R. de Sá, M. Benetti, and L. L. Graef, “An empirical investigation into cosmological tensions,” *Eur. Phys. J. Plus* **137** no. 10, (2022) 1129, [arXiv:2209.11476 \[astro-ph.CO\]](#).
- [112] S. Vagnozzi, “Consistency tests of Λ CDM from the early integrated Sachs-Wolfe effect: Implications for early-time new physics and the Hubble tension,” *Phys. Rev. D* **104** no. 6, (2021) 063524, [arXiv:2105.10425 \[astro-ph.CO\]](#).
- [113] L. Brissenden, K. Dimopoulos, and S. Sánchez López, “Non-oscillating early dark energy and quintessence from α -attractors,” *Astropart. Phys.* **157** (2024) 102925, [arXiv:2301.03572 \[astro-ph.CO\]](#).
- [114] L. Brissenden, K. Dimopoulos, and S. Sánchez López, “Explaining the Hubble tension and dark energy from alpha-attractors,” 3, 2023. [arXiv:2303.15523 \[gr-qc\]](#).
- [115] A. G. Riess *et al.*, “A Comprehensive Measurement of the Local Value of the Hubble Constant with $1 \text{ km s}^{-1} \text{ Mpc}^{-1}$ Uncertainty from the Hubble Space Telescope and the SH0ES Team,” *Astrophys. J. Lett.* **934** no. 1, (2022) L7, [arXiv:2112.04510 \[astro-ph.CO\]](#).
- [116] H. G. Escudero, J.-L. Kuo, R. E. Keeley, and K. N. Abazajian, “Early or phantom dark energy, self-interacting, extra, or massive neutrinos, primordial magnetic fields, or a curved universe: An exploration of possible solutions to the H_0 and σ_8 problems,” *Phys. Rev. D* **106** no. 10, (2022) 103517, [arXiv:2208.14435 \[astro-ph.CO\]](#).
- [117] B. S. Haridasu, H. Khoraminezhad, and M. Viel, “Scrutinizing Early Dark Energy models through CMB lensing,” [arXiv:2212.09136 \[astro-ph.CO\]](#).
- [118] R.-G. Cai, Z.-K. Guo, S.-J. Wang, W.-W. Yu, and Y. Zhou, “No-go guide for the Hubble tension: Late-time solutions,” *Phys. Rev. D* **105** no. 2, (2022) L021301, [arXiv:2107.13286 \[astro-ph.CO\]](#).
- [119] R.-G. Cai, Z.-K. Guo, S.-J. Wang, W.-W. Yu, and Y. Zhou, “No-go guide for late-time solutions to the Hubble tension: Matter perturbations,” *Phys. Rev. D* **106** no. 6, (2022) 063519, [arXiv:2202.12214 \[astro-ph.CO\]](#).
- [120] L. Knox and M. Millea, “Hubble constant hunter’s guide,” *Phys. Rev. D* **101** no. 4, (2020) 043533, [arXiv:1908.03663 \[astro-ph.CO\]](#).
- [121] A. Gómez-Valent, Z. Zheng, L. Amendola, C. Wetterich, and V. Pettorino, “Coupled and uncoupled early dark energy, massive neutrinos, and the cosmological tensions,” *Phys. Rev. D* **106** no. 10, (2022) 103522, [arXiv:2207.14487 \[astro-ph.CO\]](#).
- [122] T. Karwal and M. Kamionkowski, “Dark energy at early times, the Hubble parameter, and the string axiverse,” *Phys. Rev. D* **94** no. 10, (2016) 103523, [arXiv:1608.01309 \[astro-ph.CO\]](#).
- [123] V. Pettorino, L. Amendola, and C. Wetterich, “How early is early dark energy?,” *Phys. Rev. D* **87** (2013) 083009, [arXiv:1301.5279 \[astro-ph.CO\]](#).
- [124] E. Calabrese, D. Huterer, E. V. Linder, A. Melchiorri, and L. Pagano, “Limits on Dark Radiation, Early Dark Energy, and Relativistic Degrees of Freedom,” *Phys. Rev. D* **83** (2011) 123504, [arXiv:1103.4132 \[astro-ph.CO\]](#).
- [125] M. Doran and G. Robbers, “Early dark energy cosmologies,” *JCAP* **06** (2006) 026, [arXiv:astro-ph/0601544](#).
- [126] V. I. Sabla and R. R. Caldwell, “No H_0 assistance from assisted quintessence,” *Phys. Rev. D* **103** no. 10, (2021) 103506, [arXiv:2103.04999 \[astro-ph.CO\]](#).
- [127] T. L. Smith, V. Poulin, and M. A. Amin, “Oscillating scalar fields and the Hubble tension: a resolution with novel signatures,” *Phys. Rev. D* **101** no. 6, (2020) 063523, [arXiv:1908.06995 \[astro-ph.CO\]](#).
- [128] K. Murai, F. Naokawa, T. Namikawa, and E. Komatsu, “Isotropic cosmic birefringence from

- early dark energy,” *Phys. Rev. D* **107** no. 4, (2023) L041302, [arXiv:2209.07804 \[astro-ph.CO\]](#).
- [129] L. M. Capparelli, R. R. Caldwell, and A. Melchiorri, “Cosmic birefringence test of the Hubble tension,” *Phys. Rev. D* **101** no. 12, (2020) 123529, [arXiv:1909.04621 \[astro-ph.CO\]](#).
- [130] K. V. Berghaus and T. Karwal, “Thermal Friction as a Solution to the Hubble and Large-Scale Structure Tensions,” [arXiv:2204.09133 \[astro-ph.CO\]](#).
- [131] K. V. Berghaus and T. Karwal, “Thermal Friction as a Solution to the Hubble Tension,” *Phys. Rev. D* **101** no. 8, (2020) 083537, [arXiv:1911.06281 \[astro-ph.CO\]](#).
- [132] J. Sakstein and M. Trodden, “Early Dark Energy from Massive Neutrinos as a Natural Resolution of the Hubble Tension,” *Phys. Rev. Lett.* **124** no. 16, (2020) 161301, [arXiv:1911.11760 \[astro-ph.CO\]](#).
- [133] T. Karwal, M. Raveri, B. Jain, J. Khoury, and M. Trodden, “Chameleon early dark energy and the Hubble tension,” *Phys. Rev. D* **105** no. 6, (2022) 063535, [arXiv:2106.13290 \[astro-ph.CO\]](#).
- [134] V. I. Sabla and R. R. Caldwell, “Microphysics of early dark energy,” *Phys. Rev. D* **106** no. 6, (2022) 063526, [arXiv:2202.08291 \[astro-ph.CO\]](#).
- [135] M.-X. Lin, G. Benevento, W. Hu, and M. Raveri, “Acoustic Dark Energy: Potential Conversion of the Hubble Tension,” *Phys. Rev. D* **100** no. 6, (2019) 063542, [arXiv:1905.12618 \[astro-ph.CO\]](#).
- [136] E. McDonough and M. Scalisi, “Towards Early Dark Energy in String Theory,” [arXiv:2209.00011 \[hep-th\]](#).
- [137] V. Poulin, T. L. Smith, D. Grin, T. Karwal, and M. Kamionkowski, “Cosmological implications of ultralight axionlike fields,” *Phys. Rev. D* **98** no. 8, (2018) 083525, [arXiv:1806.10608 \[astro-ph.CO\]](#).
- [138] F. Niedermann and M. S. Sloth, “Resolving the Hubble tension with new early dark energy,” *Phys. Rev. D* **102** no. 6, (2020) 063527, [arXiv:2006.06686 \[astro-ph.CO\]](#).
- [139] J. C. Hill, E. McDonough, M. W. Toomey, and S. Alexander, “Early dark energy does not restore cosmological concordance,” *Phys. Rev. D* **102** no. 4, (2020) 043507, [arXiv:2003.07355 \[astro-ph.CO\]](#).
- [140] T. L. Smith, V. Poulin, J. L. Bernal, K. K. Boddy, M. Kamionkowski, and R. Murgia, “Early dark energy is not excluded by current large-scale structure data,” *Phys. Rev. D* **103** no. 12, (2021) 123542, [arXiv:2009.10740 \[astro-ph.CO\]](#).
- [141] S. Nojiri, S. D. Odintsov, D. Saez-Chillon Gomez, and G. S. Sharov, “Modeling and testing the equation of state for (Early) dark energy,” *Phys. Dark Univ.* **32** (2021) 100837, [arXiv:2103.05304 \[gr-qc\]](#).
- [142] V. Poulin, T. L. Smith, T. Karwal, and M. Kamionkowski, “Early Dark Energy Can Resolve The Hubble Tension,” *Phys. Rev. Lett.* **122** no. 22, (2019) 221301, [arXiv:1811.04083 \[astro-ph.CO\]](#).
- [143] K. Freese and M. W. Winkler, “Chain early dark energy: A Proposal for solving the Hubble tension and explaining today’s dark energy,” *Phys. Rev. D* **104** no. 8, (2021) 083533, [arXiv:2102.13655 \[astro-ph.CO\]](#).
- [144] P. Agrawal, F.-Y. Cyr-Racine, D. Pinner, and L. Randall, “Rock ‘n’ Roll Solutions to the Hubble Tension,” [arXiv:1904.01016 \[astro-ph.CO\]](#).
- [145] M. Braglia, W. T. Emond, F. Finelli, A. E. Gumrukcuoglu, and K. Koyama, “Unified framework for early dark energy from α -attractors,” *Phys. Rev. D* **102** no. 8, (2020) 083513, [arXiv:2005.14053 \[astro-ph.CO\]](#).

- [146] H. Moshafi, H. Firouzjahi, and A. Talebian, “Multiple Transitions in Vacuum Dark Energy and H_0 Tension,” *Astrophys. J.* **940** no. 2, (2022) 121, [arXiv:2208.05583 \[astro-ph.CO\]](#).
- [147] E. Guendelman, R. Herrera, and D. Benisty, “Unifying inflation with early and late dark energy with multiple fields: Spontaneously broken scale invariant two measures theory,” *Phys. Rev. D* **105** no. 12, (2022) 124035, [arXiv:2201.06470 \[gr-qc\]](#).
- [148] O. Seto and Y. Toda, “Comparing early dark energy and extra radiation solutions to the Hubble tension with BBN,” *Phys. Rev. D* **103** no. 12, (2021) 123501, [arXiv:2101.03740 \[astro-ph.CO\]](#).
- [149] A. Reeves, L. Herold, S. Vagnozzi, B. D. Sherwin, and E. G. M. Ferreira, “Restoring cosmological concordance with early dark energy and massive neutrinos?,” *Mon. Not. Roy. Astron. Soc.* **520** no. 3, (2023) 3688–3695, [arXiv:2207.01501 \[astro-ph.CO\]](#).
- [150] H. Mohseni Sadjadi and V. Anari, “Early dark energy and the screening mechanism,” *Eur. Phys. J. Plus* **138** no. 1, (2023) 84, [arXiv:2205.15693 \[gr-qc\]](#).
- [151] S. Goldstein, J. C. Hill, V. Iršič, and B. D. Sherwin, “Canonical Hubble-Tension-Resolving Early Dark Energy Cosmologies are Inconsistent with the Lyman- α Forest,” [arXiv:2303.00746 \[astro-ph.CO\]](#).
- [152] V. Poulin, T. L. Smith, and T. Karwal, “The Ups and Downs of Early Dark Energy solutions to the Hubble tension: a review of models, hints and constraints circa 2023,” [arXiv:2302.09032 \[astro-ph.CO\]](#).
- [153] J. a. Rebouças, J. Gordon, D. H. F. de Souza, K. Zhong, V. Miranda, R. Rosenfeld, T. Eifler, and E. Krause, “Early dark energy constraints with late-time expansion marginalization,” [arXiv:2302.07333 \[astro-ph.CO\]](#).
- [154] J. S. Cruz, S. Hannestad, E. B. Holm, F. Niedermann, M. S. Sloth, and T. Tram, “Profiling Cold New Early Dark Energy,” [arXiv:2302.07934 \[astro-ph.CO\]](#).
- [155] M. Carrillo González, Q. Liang, J. Sakstein, and M. Trodden, “Neutrino-Assisted Early Dark Energy is a Natural Resolution of the Hubble Tension,” [arXiv:2302.09091 \[astro-ph.CO\]](#).
- [156] J. R. Eskilt, L. Herold, E. Komatsu, K. Murai, T. Namikawa, and F. Naokawa, “Constraint on Early Dark Energy from Isotropic Cosmic Birefringence,” [arXiv:2303.15369 \[astro-ph.CO\]](#).
- [157] S. D. Odintsov, V. K. Oikonomou, and G. S. Sharov, “Early dark energy with power-law $F(R)$ gravity,” *Phys. Lett. B* **843** (2023) 137988, [arXiv:2305.17513 \[gr-qc\]](#).
- [158] E. J. Copeland, A. Moss, S. Sevilano Muñoz, and J. M. M. White, “Scaling solutions as Early Dark Energy resolutions to the Hubble tension,” [arXiv:2309.15295 \[astro-ph.CO\]](#).
- [159] M. Raveri, “Resolving the Hubble tension at late times with Dark Energy,” [arXiv:2309.06795 \[astro-ph.CO\]](#).
- [160] R. K. Sharma, S. Das, and V. Poulin, “Early Dark Energy beyond slow-roll: implications for cosmic tensions,” [arXiv:2309.00401 \[astro-ph.CO\]](#).
- [161] H. B. Benaoum, L. A. García, and L. Castañeda, “Early dark energy induced by non-linear electrodynamics,” [arXiv:2307.05917 \[gr-qc\]](#).
- [162] F. Niedermann and M. S. Sloth, “New Early Dark Energy as a solution to the H_0 and S_8 tensions,” [arXiv:2307.03481 \[hep-ph\]](#).
- [163] T. Kodama, T. Shinohara, and T. Takahashi, “Generalized early dark energy and its cosmological consequences,” [arXiv:2309.11272 \[astro-ph.CO\]](#).
- [164] S. Vagnozzi, “Seven hints that early-time new physics alone is not sufficient to solve the Hubble tension,” *Universe* **9** (2023) 393, [arXiv:2308.16628 \[astro-ph.CO\]](#).
- [165] M. Cicoli, M. Licheri, R. Mahanta, E. McDonough, F. G. Pedro, and M. Scalisi, “Early Dark Energy in Type IIB String Theory,” *JHEP* **06** (2023) 052, [arXiv:2303.03414 \[hep-th\]](#).

- [166] L. Kofman, A. D. Linde, X. Liu, A. Maloney, L. McAllister, and E. Silverstein, “Beauty is attractive: Moduli trapping at enhanced symmetry points,” *JHEP* **05** (2004) 030, [arXiv:hep-th/0403001](#).
- [167] K. Dimopoulos, M. Karčiauskas, and C. Owen, “Quintessential inflation with a trap and axionic dark matter,” *Phys. Rev. D* **100** no. 8, (2019) 083530, [arXiv:1907.04676 \[hep-ph\]](#).
- [168] A. Sarkar and B. Ghosh, “Constraining the quintessential α -attractor inflation through dynamical horizon exit method,” *Phys. Dark Univ.* **41** (2023) 101239, [arXiv:2305.00230 \[gr-qc\]](#).
- [169] A. Sarkar, C. Sarkar, and B. Ghosh, “A novel way of constraining the α -attractor chaotic inflation through Planck data,” *JCAP* **11** no. 11, (2021) 029, [arXiv:2106.02920 \[gr-qc\]](#).
- [170] C. Wetterich, “Quintessenz – die fünfte Kraft,” *Physik J.* **3N12** (2004) 43–48.
- [171] A. Linde, “On the problem of initial conditions for inflation,” *Found. Phys.* **48** no. 10, (2018) 1246–1260, [arXiv:1710.04278 \[hep-th\]](#).
- [172] R. Kallosh and A. Linde, “Cosmological Attractors and Asymptotic Freedom of the Inflaton Field,” *JCAP* **06** (2016) 047, [arXiv:1604.00444 \[hep-th\]](#).
- [173] J. Chojnacki, J. Krajecka, J. H. Kwapisz, O. Slowik, and A. Strag, “Is asymptotically safe inflation eternal?,” *JCAP* **04** (2021) 076, [arXiv:2101.00866 \[gr-qc\]](#).
- [174] R. Kallosh, A. Linde, and D. Roest, “Superconformal Inflationary α -Attractors,” *JHEP* **11** (2013) 198, [arXiv:1311.0472 \[hep-th\]](#).
- [175] S. Ferrara, R. Kallosh, A. Linde, and M. Porrati, “Minimal Supergravity Models of Inflation,” *Phys. Rev. D* **88** no. 8, (2013) 085038, [arXiv:1307.7696 \[hep-th\]](#).
- [176] R. Kallosh and A. Linde, “Superconformal generalization of the chaotic inflation model $\frac{\lambda}{4}\phi^4 - \frac{\xi}{2}\phi^2 R$,” *JCAP* **06** (2013) 027, [arXiv:1306.3211 \[hep-th\]](#).
- [177] R. Kallosh and A. Linde, “Non-minimal Inflationary Attractors,” *JCAP* **10** (2013) 033, [arXiv:1307.7938 \[hep-th\]](#).
- [178] R. Kallosh and A. Linde, “Planck, LHC, and α -attractors,” *Phys. Rev. D* **91** (2015) 083528, [arXiv:1502.07733 \[astro-ph.CO\]](#).
- [179] J. J. M. Carrasco, R. Kallosh, and A. Linde, “ α -Attractors: Planck, LHC and Dark Energy,” *JHEP* **10** (2015) 147, [arXiv:1506.01708 \[hep-th\]](#).
- [180] R. Kallosh and A. Linde, “Universality Class in Conformal Inflation,” *JCAP* **07** (2013) 002, [arXiv:1306.5220 \[hep-th\]](#).
- [181] K.-I. Maeda, S. Mizuno, and R. Tozuka, “ α -attractor-type double inflation,” *Phys. Rev. D* **98** no. 12, (2018) 123530, [arXiv:1810.06914 \[hep-th\]](#).
- [182] R. Kallosh, A. Linde, and D. Roest, “Large field inflation and double α -attractors,” *JHEP* **08** (2014) 052, [arXiv:1405.3646 \[hep-th\]](#).
- [183] M. Galante, R. Kallosh, A. Linde, and D. Roest, “Unity of Cosmological Inflation Attractors,” *Phys. Rev. Lett.* **114** no. 14, (2015) 141302, [arXiv:1412.3797 \[hep-th\]](#).
- [184] R. Kallosh, A. Linde, and D. Roest, “Universal Attractor for Inflation at Strong Coupling,” *Phys. Rev. Lett.* **112** no. 1, (2014) 011303, [arXiv:1310.3950 \[hep-th\]](#).
- [185] S. Ferrara, R. Kallosh, A. Linde, and M. Porrati, “Higher Order Corrections in Minimal Supergravity Models of Inflation,” *JCAP* **11** (2013) 046, [arXiv:1309.1085 \[hep-th\]](#).
- [186] A. Linde, D.-G. Wang, Y. Welling, Y. Yamada, and A. Achúcarro, “Hypernatural inflation,” *JCAP* **07** (2018) 035, [arXiv:1803.09911 \[hep-th\]](#).
- [187] S. Cecotti and R. Kallosh, “Cosmological Attractor Models and Higher Curvature Supergravity,” *JHEP* **05** (2014) 114, [arXiv:1403.2932 \[hep-th\]](#).

- [188] S. Ferrara, P. Fré, and A. S. Sorin, “On the Topology of the Inflaton Field in Minimal Supergravity Models,” *JHEP* **04** (2014) 095, [arXiv:1311.5059 \[hep-th\]](#).
- [189] S. Ferrara, P. Fre, and A. S. Sorin, “On the Gauged Kähler Isometry in Minimal Supergravity Models of Inflation,” *Fortsch. Phys.* **62** (2014) 277–349, [arXiv:1401.1201 \[hep-th\]](#).
- [190] K. Dasgupta, M. Emelin, E. McDonough, and R. Tatar, “Quantum Corrections and the de Sitter Swampland Conjecture,” *JHEP* **01** (2019) 145, [arXiv:1808.07498 \[hep-th\]](#).
- [191] A. Let, A. Sarkar, C. Sarkar, and B. Ghosh, “Single-field slow-roll effective potential from Kähler moduli stabilizations in type-IIB/F-theory,” *EPL* **139** no. 5, (2022) 59002, [arXiv:2208.06606 \[hep-th\]](#).
- [192] A. Let, A. Sarkar, C. Sarkar, and B. Ghosh, “Non-perturbative stabilization of two Kähler moduli in type-IIB/F theory and the inflaton potential,” *EPL* **143** no. 3, (2023) 39001, [arXiv:2308.00302 \[gr-qc\]](#).
- [193] J. J. M. Carrasco, R. Kallosh, and A. Linde, “Cosmological Attractors and Initial Conditions for Inflation,” *Phys. Rev. D* **92** no. 6, (2015) 063519, [arXiv:1506.00936 \[hep-th\]](#).
- [194] R. Kallosh and A. Linde, “Escher in the Sky,” *Comptes Rendus Physique* **16** (2015) 914–927, [arXiv:1503.06785 \[hep-th\]](#).
- [195] J. J. M. Carrasco, R. Kallosh, A. Linde, and D. Roest, “Hyperbolic geometry of cosmological attractors,” *Phys. Rev. D* **92** no. 4, (2015) 041301, [arXiv:1504.05557 \[hep-th\]](#).
- [196] R. Kallosh, A. Linde, T. Wrase, and Y. Yamada, “Maximal Supersymmetry and B-Mode Targets,” *JHEP* **04** (2017) 144, [arXiv:1704.04829 \[hep-th\]](#).
- [197] S. D. Odintsov and V. K. Oikonomou, “Inflationary α -attractors from $F(R)$ gravity,” *Phys. Rev. D* **94** no. 12, (2016) 124026, [arXiv:1612.01126 \[gr-qc\]](#).
- [198] M. Scalisi and I. Valenzuela, “Swampland distance conjecture, inflation and α -attractors,” *JHEP* **08** (2019) 160, [arXiv:1812.07558 \[hep-th\]](#).
- [199] R. Kallosh, A. Linde, D. Roest, A. Westphal, and Y. Yamada, “Fibre Inflation and α -attractors,” *JHEP* **02** (2018) 117, [arXiv:1707.05830 \[hep-th\]](#).
- [200] R. Kallosh, A. Linde, T. Wrase, and Y. Yamada, “IIB String Theory and Sequestered Inflation,” *Fortsch. Phys.* **69** no. 11-12, (2021) 2100127, [arXiv:2108.08492 \[hep-th\]](#).
- [201] R. Kallosh and A. Linde, “CMB targets after the latest Planck data release,” *Phys. Rev. D* **100** no. 12, (2019) 123523, [arXiv:1909.04687 \[hep-th\]](#).
- [202] R. Kallosh and A. Linde, “B-mode Targets,” *Phys. Lett. B* **798** (2019) 134970, [arXiv:1906.04729 \[astro-ph.CO\]](#).
- [203] S. Ferrara and R. Kallosh, “Seven-disk manifold, α -attractors, and B modes,” *Phys. Rev. D* **94** no. 12, (2016) 126015, [arXiv:1610.04163 \[hep-th\]](#).
- [204] K. Dimopoulos, L. Donaldson Wood, and C. Owen, “Instant preheating in quintessential inflation with α -attractors,” *Phys. Rev. D* **97** no. 6, (2018) 063525, [arXiv:1712.01760 \[astro-ph.CO\]](#).
- [205] D. Baumann, “Inflation,” in *Theoretical Advanced Study Institute in Elementary Particle Physics: Physics of the Large and the Small*, pp. 523–686. 2011. [arXiv:0907.5424 \[hep-th\]](#).
- [206] D. Baumann, *Cosmology*. Cambridge University Press, 7, 2022.
- [207] E. J. Copeland, A. R. Liddle, and D. Wands, “Exponential potentials and cosmological scaling solutions,” *Phys. Rev. D* **57** (1998) 4686–4690, [arXiv:gr-qc/9711068](#).
- [208] S. Dodelson, “Coherent phase argument for inflation,” *AIP Conf. Proc.* **689** no. 1, (2003) 184–196, [arXiv:hep-ph/0309057](#).

- [209] N. Bartolo, S. Matarrese, and A. Riotto, “Adiabatic and isocurvature perturbations from inflation: Power spectra and consistency relations,” *Phys. Rev. D* **64** (2001) 123504, [arXiv:astro-ph/0107502](#).
- [210] C. Gordon, D. Wands, B. A. Bassett, and R. Maartens, “Adiabatic and entropy perturbations from inflation,” *Phys. Rev. D* **63** (2000) 023506, [arXiv:astro-ph/0009131](#).
- [211] N. Bartolo, E. Komatsu, S. Matarrese, and A. Riotto, “Non-Gaussianity from inflation: Theory and observations,” *Phys. Rept.* **402** (2004) 103–266, [arXiv:astro-ph/0406398](#).
- [212] V. Acquaviva, N. Bartolo, S. Matarrese, and A. Riotto, “Second order cosmological perturbations from inflation,” *Nucl. Phys. B* **667** (2003) 119–148, [arXiv:astro-ph/0209156](#).
- [213] J. M. Maldacena, “Non-Gaussian features of primordial fluctuations in single field inflationary models,” *JHEP* **05** (2003) 013, [arXiv:astro-ph/0210603](#).
- [214] E. Komatsu and D. N. Spergel, “Acoustic signatures in the primary microwave background bispectrum,” *Phys. Rev. D* **63** (2001) 063002, [arXiv:astro-ph/0005036](#).
- [215] D. I. Kaiser, E. A. Mazenc, and E. I. Sfakianakis, “Primordial Bispectrum from Multifield Inflation with Nonminimal Couplings,” *Phys. Rev. D* **87** (2013) 064004, [arXiv:1210.7487 \[astro-ph.CO\]](#).
- [216] T. S. Bunch and P. C. W. Davies, “Quantum Field Theory in de Sitter Space: Renormalization by Point Splitting,” *Proc. Roy. Soc. Lond. A* **360** (1978) 117–134.
- [217] N. D. Birrell and P. C. W. Davies, *Quantum Fields in Curved Space*. Cambridge Monographs on Mathematical Physics. Cambridge Univ. Press, Cambridge, UK, 2, 1984.
- [218] S. Kundu, “Inflation with General Initial Conditions for Scalar Perturbations,” *JCAP* **02** (2012) 005, [arXiv:1110.4688 \[astro-ph.CO\]](#).
- [219] H. Jiang, Y. Wang, and S. Zhou, “On the initial condition of inflationary fluctuations,” *JCAP* **04** (2016) 041, [arXiv:1601.01179 \[hep-th\]](#).
- [220] M. Tristram *et al.*, “Improved limits on the tensor-to-scalar ratio using BICEP and Planck data,” *Phys. Rev. D* **105** no. 8, (2022) 083524, [arXiv:2112.07961 \[astro-ph.CO\]](#).
- [221] **QUaD** Collaboration, M. L. Brown *et al.*, “Improved measurements of the temperature and polarization of the CMB from QUaD,” *Astrophys. J.* **705** (2009) 978–999, [arXiv:0906.1003 \[astro-ph.CO\]](#).
- [222] **QUIET** Collaboration, D. Araujo *et al.*, “Second Season QUIET Observations: Measurements of the CMB Polarization Power Spectrum at 95 GHz,” *Astrophys. J.* **760** (2012) 145, [arXiv:1207.5034 \[astro-ph.CO\]](#).
- [223] **SPT** Collaboration, J. T. Sayre *et al.*, “Measurements of B-mode Polarization of the Cosmic Microwave Background from 500 Square Degrees of SPTpol Data,” *Phys. Rev. D* **101** no. 12, (2020) 122003, [arXiv:1910.05748 \[astro-ph.CO\]](#).
- [224] **ACTPol** Collaboration, S. Naess *et al.*, “The Atacama Cosmology Telescope: CMB Polarization at $200 < \ell < 9000$,” *JCAP* **10** (2014) 007, [arXiv:1405.5524 \[astro-ph.CO\]](#).
- [225] **SPT** Collaboration, R. Keisler *et al.*, “Measurements of Sub-degree B-mode Polarization in the Cosmic Microwave Background from 100 Square Degrees of SPTpol Data,” *Astrophys. J.* **807** no. 2, (2015) 151, [arXiv:1503.02315 \[astro-ph.CO\]](#).
- [226] S. W. Henderson *et al.*, “Advanced ACTPol Cryogenic Detector Arrays and Readout,” *J. Low Temp. Phys.* **184** no. 3-4, (2016) 772–779, [arXiv:1510.02809 \[astro-ph.IM\]](#).
- [227] **SPT-3G** Collaboration, B. A. Benson *et al.*, “SPT-3G: A Next-Generation Cosmic Microwave Background Polarization Experiment on the South Pole Telescope,” *Proc. SPIE Int. Soc. Opt. Eng.* **9153** (2014) 91531P, [arXiv:1407.2973 \[astro-ph.IM\]](#).

- [228] **LiteBIRD** Collaboration, M. Hazumi *et al.*, “LiteBIRD: JAXA’s new strategic L-class mission for all-sky surveys of cosmic microwave background polarization,” *Proc. SPIE Int. Soc. Opt. Eng.* **11443** (2020) 114432F, [arXiv:2101.12449 \[astro-ph.IM\]](#).
- [229] C. Heymans *et al.*, “CFHTLenS: The Canada-France-Hawaii Telescope Lensing Survey,” *Mon. Not. Roy. Astron. Soc.* **427** (2012) 146, [arXiv:1210.0032 \[astro-ph.CO\]](#).
- [230] H. Hildebrandt *et al.*, “KiDS-450: Cosmological parameter constraints from tomographic weak gravitational lensing,” *Mon. Not. Roy. Astron. Soc.* **465** (2017) 1454, [arXiv:1606.05338 \[astro-ph.CO\]](#).
- [231] F. Köhlinger *et al.*, “KiDS-450: The tomographic weak lensing power spectrum and constraints on cosmological parameters,” *Mon. Not. Roy. Astron. Soc.* **471** no. 4, (2017) 4412–4435, [arXiv:1706.02892 \[astro-ph.CO\]](#).
- [232] K. S. Dawson *et al.*, “The SDSS-IV extended Baryon Oscillation Spectroscopic Survey: Overview and Early Data,” *Astron. J.* **151** (2016) 44, [arXiv:1508.04473 \[astro-ph.CO\]](#).
- [233] **DES** Collaboration, T. Abbott *et al.*, “Cosmology from cosmic shear with Dark Energy Survey Science Verification data,” *Phys. Rev. D* **94** no. 2, (2016) 022001, [arXiv:1507.05552 \[astro-ph.CO\]](#).
- [234] **DESI** Collaboration, A. Aghamousa *et al.*, “The DESI Experiment Part I: Science, Targeting, and Survey Design,” [arXiv:1611.00036 \[astro-ph.IM\]](#).
- [235] **DESI** Collaboration, A. Aghamousa *et al.*, “The DESI Experiment Part II: Instrument Design,” [arXiv:1611.00037 \[astro-ph.IM\]](#).
- [236] **LSST Science, LSST Project** Collaboration, P. A. Abell *et al.*, “LSST Science Book, Version 2.0,” [arXiv:0912.0201 \[astro-ph.IM\]](#).
- [237] **LSST** Collaboration, P. Marshall *et al.*, “Science-Driven Optimization of the LSST Observing Strategy,” [arXiv:1708.04058 \[astro-ph.IM\]](#).
- [238] D. Spergel *et al.*, “Wide-Field Infrared Survey Telescope-Astrophysics Focused Telescope Assets WFIRST-AFTA 2015 Report,” [arXiv:1503.03757 \[astro-ph.IM\]](#).
- [239] R. Hounsell *et al.*, “Simulations of the WFIRST Supernova Survey and Forecasts of Cosmological Constraints,” *Astrophys. J.* **867** no. 1, (2018) 23, [arXiv:1702.01747 \[astro-ph.IM\]](#).
- [240] L. Amendola *et al.*, “Cosmology and fundamental physics with the Euclid satellite,” *Living Rev. Rel.* **21** no. 1, (2018) 2, [arXiv:1606.00180 \[astro-ph.CO\]](#).